1954

Low temperature heat capacities of thorium, gadolinium and erbium

Richard Ernest Skochdopole
Iowa State College

Recommended Citation

Skochdopole, Richard Ernest, "Low temperature heat capacities of thorium, gadolinium and erbium " (1954). *Retrospective Theses and Dissertations*. 12927.
https://lib.dr.iastate.edu/rtd/12927

UNCLASSIFIED

Title: Low Temperature Heat Capacities of Thorium, Gadolinium and Erbium

Author: Richard Skochdopole

(Official certification of the classification shown is filed in the Ames Laboratory Document Library)

Signature was redacted for privacy.

W. E. Dreeszen

Secretary to Declassification
Committee

UNCLASSIFIED

LOW TEMPERATURE HEAT CAPACITIES OF THORIUM, GADOLINIUM AND ERBIUM

by

Richard E. Skochdopole

A Dissertation Submitted to the
Graduate Faculty in Partial Fulfillment of
The Requirements for the Degree of
DOCTOR OF PHILOSOPHY

Major Subject: Physical Chemistry

Approved:

Signature was redacted for privacy.

Signature was redacted for privacy.

In Charge of Major Work

Signature was redacted for privacy.

Head of Major Department

Signature was redacted for privacy.

Dean of Graduate College

Iowa State College

1954

ProQuest Information and Learning Company
300 North Zeeb Road
P.O. Box 1346
Ann Arbor, MI 48106-1346

TABLE OF CONTENTS

INTRODUCTION

Interest in the investigation of the heat capacity of a substance over the temperature range 15 to 300°K. may arise from any one of several reasons. The most obvious of these is that from such data there can be calculated the various thermodynamic functions; in particular, the entropy and the free energy function. Aside from such utilitarian considerations, the behavior of the heat capacity provides information on the nature of certain processes which occur as the temperature is raised. The most important such process, that of vibrational excitation of the lattice, has received much attention both experimentally and theoretically and remains to this day a field of active interest.[1]

In addition to this ever present or "normal" effect of lattice vibration, there may exist other phenomena with which an energy change is associated and which appear as anomalies on the otherwise normal heat capacity curve. The temperature at which an anomalous energy change is most rapid is immediately evident. If, in addition, it is possible to separate the normal and anomalous contributions to the heat capacity, then the energy and entropy changes associated with each may be calculated. Some examples of phenomena which have been studied in this manner are: phase or structure changes, order-disorder effects, magnetic transitions, electronic transitions, and hindered rotation in molecules.

The heat capacity of adsorbed gases has recently received increased attention.

The objective of this research was the determination of the heat capacities of some of the metals of the lanthanide and actinide series which have recently become available. The approximate temperature range of these measurements was 15-300°K. The proposed measurements were of interest because: the heat capacities and thermodynamic functions of these metals were unknown; the lanthanides, or rare earths, have long been subjects for magnetic studies; and a comparison of the heat capacities among members of each group, as well as comparison with corresponding members of the other series, was desired. The metals thorium, gadolinium, and erbium were chosen for this study.

The principal reason for measuring the heat capacity of thorium was to obtain the thermodynamic functions. A value of $S^{o}_{298.16} = 13.58$ was estimated by Lewis and Gibson[2] in 1917 and had not been further checked. As the entropy is a quantity widely used in chemical thermodynamic calculations, it seemed advisable to determine it accurately. Cerium is the element in the lanthanide series corresponding to thorium in the actinide series. The low temperature heat capacity of cerium[3] exhibits anomalies which are attributed to the behavior of its 4 f electron, and the measurements proposed here would show whether this anomalous behavior carries over to the 5 f electron of thorium.

The choice of gadolinium for heat capacity measurements seemed advantageous for several reasons. The heat capacity and thermodynamic functions were previously unknown, and these would be of value in any consideration of the chemical or metallurgical properties. Gadolinium has also been the subject of extensive magnetic study since it was discovered to be the fourth ferromagnetic element.[4] That an enhanced heat capacity is associated with ferromagnetism is well known, and the investigation of the magnetic contribution to the heat capacity is of interest in confronting theories of ferromagnetism. The Curie temperature of 16°C. for gadolinium, in contrast to the high Curie temperatures of the other ferromagnetic elements, occurs in a range well suited for accurate measurement of heat capacity.

The heat capacity and thermodynamic functions of erbium, like gadolinium, were unknown. Erbium also has been the subject of considerable study, but without such definite conclusions as in the case of gadolinium. Néel[5] proposed that erbium would be ferromagnetic with a Curie temperature of 40°K. Recent studies of the magnetic susceptibility and neutron diffraction, however, have indicated that its magnetic behavior below 80°K. is complex and the results of these experiments are not completely understood. Since the low temperature anomalies that exist in the heat capacities of cerium and neodymium[3] can be attributed to the behavior of the 4 f electrons, it seemed probable that similar anomalies might occur in the case of erbium. It was hoped that the investigation of the heat capacity of erbium would provide information about the exact temperature and the entropy associated with the magnetic and possible electronic transitions. Such information should be valuable in the interpretation and understanding of these phenomena.

REVIEW OF LITERATURE

Thorium

The value of $S^{o}_{298.16} = 13.58$ for thorium was estimated by Lewis and Gibson[2] in 1917. It was based on the measurement by Dewar[6] of the average value of the atomic heat of thorium between the temperatures of liquid hydrogen and liquid nitrogen. This approximate value of the entropy had not been further checked and is presented in the standard compilations of Kelley[7] and of the National Bureau of Standards.[8]

The heat capacity measurements on cerium by Parkinson, Simon, and Spedding[3] were used in the comparison with the heat capacity of thorium. They found that cerium possesses two anomalous regions in its heat capacity, one from 90-180°K. and the other in the neighborhood of 12°K. They associated the anomaly in the 90-180°K. range with the appearance of a condensed phase in cerium, which probably occurs with the promotion of one 4 f electron to a 5 d state.[9,10] The anomaly in the region around 12°K. also appears to be associated with the 4 f electron, but is of a very complex nature.[3,11]

Gadolinium

Urbain, Weiss, and Trombe[4] first reported gadolinium to be the fourth ferromagnetic element, with a Curie temperature of 16°C. ± 2°.

Later magnetic work by Trombe[12] and by Elliott, Legvold, and Spedding[13] has confirmed their results.

Other studies having a bearing on the ferromagnetic behavior of gadolinium include dilatometric measurements by Barson, Legvold, and Spedding[14] and Trombe and Foex.[15] The results of these two investigations did not agree, but this was probably due to the questionable state of the sample in the case of the former. Legvold, Spedding, Barson, and Elliott[16] investigated the electrical resistivity from 4-360°K. and found an abrupt change in the temperature versus resistivity curve at around 300°K. Kevane, Legvold, and Spedding[17] reported measurements of the Hall effect from 303-623°K. Banister, Legvold, and Spedding[18] have measured the temperature variation of the lattice parameters from 48-300°K. by means of X-rays. They found that the structure of gadolinium remains hexagonal closest-packed over the entire temperature range. An approximate calculation of the linear coefficient of expansion from their work agrees well with the dilatometric measurements of Trombe and Foex.[15]

Erbium

Néel[5] estimated that erbium would be ferromagnetic with a Curie temperature of 40°K. A recent study of the magnetic susceptibility in the range 20-71°K. has been made by Elliott, Legvold, and Spedding.[13] They found that the magnetic susceptibility becomes field dependent at 56°K. ± 5°, and that erbium is apparently ferromagnetic below 20°K. Between these temperatures the field dependence becomes more pronounced as the temperature decreases. The same authors extended the magnetic susceptibility measurements from 70-90°K.[19] These measurements showed that there exists a region of almost complete temperature independence of the susceptibility between 65-80°K., with a slight maximum at 80°K. This behavior was likened to that of an antiferromagnet. Preliminary results from neutron diffraction measurements by Kohler and Wollan[20] were quite complex and difficult to interpret. They gave strong evidence for the existence of a ferromagnetic state at 4°K. and also showed what appeared to be various degrees of magnetic ordering in the range 4-78°K.

Other work having some bearing on the magnetic behavior of erbium includes that on electrical resistivity by Legvold, *et al*.[16] in the range 4-280°K. They found a small change in the slope of the resistivity versus temperature curve at about 80°K. Hall effect measurements from 100-300°K. by Kevane, Legvold, and Spedding[17] showed a gradual rise of the Hall coefficient as the temperature is decreased. Dilatometric measurements in the range 100-300°K. have been reported by Barson, Legvold, and Spedding.[14] Banister, Legvold, and Spedding[18] have measured the lattice parameters between 40-300°K. They found that erbium is hexagonal closest-packed over the entire range studied. A value for the linear expansion coefficient calculated from this work agrees fairly well with that of Barson, Legvold, and Spedding.[14]

MATERIALS AND APPARATUS

Materials

Thorium

The thorium sample was in the form of a right circular cylinder three inches in length and 1.5 inches in diameter. It was extruded thorium prepared by the Ames Laboratory and weighed 954.066 g. *in vacuo*, which was equivalent to 4.1102 g. atoms. Chemical analysis showed it to contain 0.025 per cent silicon with aluminum, calcium, iron, magnesium, and zinc present to, at most, 100 parts per million. Vacuum fusion analysis by the National Research Corporation showed it to contain 0.04 per cent nitrogen and 0.06 per cent oxygen.

Gadolinium

The gadolinium sample was in the form of a right circular cylinder 2.59 inches in length and 1.44 inches in diameter. It weighed 505.290 g. *in vacuo*, which was equivalent to 3.2205 g. atoms. The metal was prepared by reduction with calcium of the anhydrous fluoride. Procedures for the ion exchange separation of the gadolinium and for the reduction were developed previously at Iowa State College.[21,22] Ten buttons of metal were made and recast *in vacuo* in a tantalum crucible, during which process the excess calcium was distilled off. The tantalum was then either stripped off or machined off the casting. Spectrographic analysis showed it to contain approximately 0.1 per cent samarium, less than 0.1 per cent yttrium, less than 0.3 per cent tantalum, and less than 0.04 per cent calcium. Silicon, iron, and magnesium were present to less than 0.01 per cent. Other rare earths were not detected.

Erbium

The erbium metal was prepared by reduction with calcium of the anhydrous fluoride. Procedures for the ion exchange separation and subsequent reduction had been previously developed at Iowa State College. Due to the low boiling point of erbium, the casting together of the several small buttons and accompanying distillation separation of the excess calcium was done in an argon atmosphere rather than *in vacuo*. After the tantalum crucible had been machined off, the sample was 2.95 inches in length and 1.22 inches in diameter with a weight of 429.58 g., which was equivalent to 2.5680 g. atoms.

A spectrographic analysis of the erbium showed less than 0.01 per cent calcium, magnesium, silicon, and yttrium. The other rare earths, iron, and tantalum were not detected. Perhaps it should be noted that a method of analysis for oxygen and nitrogen in erbium and gadolinium was not available at the time. It was almost certain that small amounts of these elements were present in adsorbed or combined condition.

Apparatus

Mechanical features

The adiabatic calorimeter schematically represented in Figure 1 was similar in design to that of Blue and Hicks.[23] It was built so that future modification could include the windlass design of Ruehrwein and Huffman.[24]

In the cases of thorium and gadolinium, containers were not used for the samples. Instead the metal cylinder or "block" was directly suspended inside the shield by nylon cords. In each case, a hole was made along the axis of the sample to accommodate the heater shell. The thermometer then fit snugly inside the heater shell. The thermocouple holders plus heater and thermocouple rings were attached to the block with 00-90 screws and holes tapped directly into the sample. Apiezon T grease was used to improve thermal contact of metal-metal joints. Figure 2 shows an enlarged view of the calorimeter chamber with the calorimeter can in place.

Since it was found that the gadolinium block was able to maintain quite large thermal gradients during heating periods, the erbium sample was placed in a gold-plated copper can. The erbium sample, in the shape of a metal cylinder, had a hole machined along its axis, such that it made a snug fit over the reentrant well of the can. The reentrant well was made to accommodate the heater shell, which in turn housed the thermometer. Thermal contact was aided by Apiezon T grease and helium exchange gas.

Figure 1

Adiabatic calorimeter

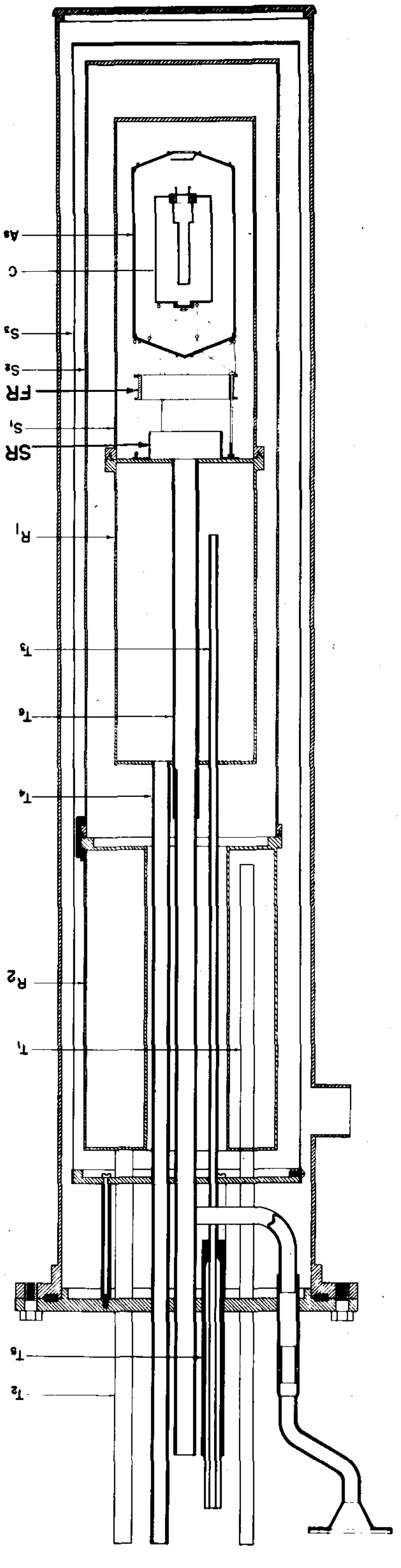
A_s
C
S_3
S_2
FR
S_1
SR
R_1
T_3
T_6
T_4
R_2
T_1
T_5
T_2

Figure 2

Calorimeter chamber

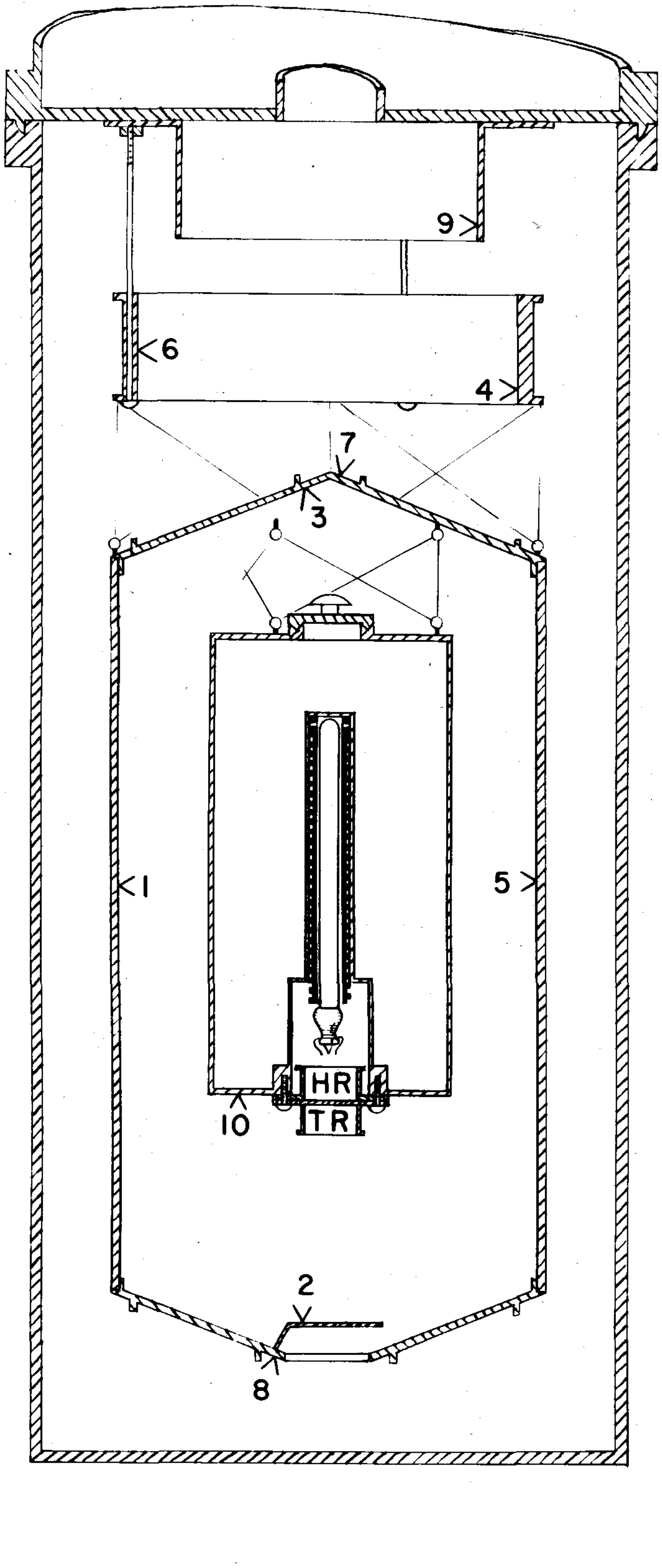
9
6
4
7
3
1
5
HR
TR
10
2
8

The bottom of the can was attached with 50-50 Sn-Pb solder and the top of the can was attached with low-melting indium solder. An exchange gas port, consisting of a thin walled .066 inch O.D. copper tube with a flange, was soldered to the top of the can with Sn-Pb solder.

Surrounding the calorimeter proper was the adiabatic shield, AS. This was provided with separate heaters on the top, bottom, and side which were used to control the temperature of the shield as closely as possible to the temperature of the calorimeter proper. In this manner, the heat exchange between the sample and its environment was minimized. The adiabatic shield, AS, was made in three pieces: a cylindrical body closed at each end by a conical cap. Henceforth, the cylindrical body of the block, calorimeter can, and adiabatic shield will be referred to as the side in order to simplify nomenclature. The bottom cone had a 3/8 inch hole through the center for easy evacuation; direct radiation was intercepted by a baffle plate. The three pieces fit snugly, with the top and bottom each being bolted to the side with three 1-72 screws. The adiabatic shield was suspended by nylon cord from the "floating ring," FR. The floating ring was suspended by three 0-80 stainless steel screws which fit into small lugs on the stationary ring, SR. The latter was soldered to the bottom of the lower reservoir, R_1. Surrounding this assembly was the shield, S_1, which was in thermal contact with the lower reservoir. The joint between the shield and the reservoir was of the bayonet type, a vacuum seal being made by an indium-based solder. Surrounding this assembly was the combination of the annular-shaped upper reservoir, R_2, and its associated shield, S_2. Since the bayonet type seal between these two did not need to be vacuum-tight, steel clips were used to fasten the joint. Thermal contact between the shield and reservoir was improved by having stopcock grease in the bayonet well. Surrounding the upper reservoir and its shield was a floating shield, S_3, so called because it assumed a temperature intermediate between that of S_2 and the outer brass container. The floating shield, S_3, was fastened to a monel plate which was penetrated by all of the filling and pumping tubes. This monel plate was in turn rigidly suspended from the brass cover plate of the cryostat by three steel screws 3½ inches long. Correct alignment and vertical spacing was maintained by three bushings 3 1/8 inches long. The entire assembly fit into a brass can of the following dimensions: 7¼ inches O.D., 35½ inches in length, 1/8 inch wall. The central pumping tube for the calorimeter chamber, as well as the hydrogen tank filling and exit tubes, went down through the annulus of the upper reservoir. The central pumping tube continued through the lower reservoir.

All shields and reservoirs were chromium-plated except the adiabatic shield, AS, which was gold-plated. The various filling and pumping tubes were soft soldered into the cover plate of the cryostat and served to support the entire assembly. The cover plate and the flange on the brass cryostat each had a carefully machined groove to accommodate an O-ring so that a vacuum seal could be made. The brass can was provided with a one inch side port for evacuation by a two-stage oil diffusion pump. The chamber inside of S_1 had a separate and similar vacuum system.

The entire inner assembly could be lifted by a hoist. Two rods

½ inch in diameter screwed into the cryostat cover and were connected at the top by a cross bar to which a hoist might be attached. The mechanical details of these parts are summarized in Table 1.

Table 1

Materials

Cryostat can:	Seamless brass tube; 35½" high; 7¼" O.D.; 1/8" wall
Cryostat flange:	Brass 9 5/8" O.D.; thickness 5/16"; shoulder ½"
Cryostat cover:	Brass 9 5/8" O.D.; thickness 3/8"
Floating shield: S_3	Copper 0.010" thick; 6½" O.D.
Upper reservoir: R_2	Copper tube 5½" O.D.; 1/16" wall
	Copper tube 2½" O.D.; 1/16" wall
U. reservoir shield: S_2	Copper tube 5½" O.D.; 1/16" wall
Lower reservoir: R_1	Copper tube 4" O.D.; 1/16" wall
L. reservoir shield: S_1	Copper tube 4" O.D.; 1/16" wall
U. reservoir filling tube: T_1	Monel 3/8" O.D.; 0.016" wall
U. reservoir pumping tube: T_2	Monel ½" O.D.; 0.032" wall
L. reservoir filling tube: T_3	Monel ¼" O.D.; 0.032" wall
L. reservoir pumping tube: T_4	Monel ½" O.D.; 0.032" wall
Transfer guide tube: T_5	Brass 5/8" O.D.; 1/16" wall
Central pumping tube: T_6	Upper, monel 5/8" O.D.; 0.032" wall Lower, copper 3/4" O.D.; 0.032" wall

The transfer tube for the lower reservoir was demountable. A rubber seal was made at the top of the guide tube so that it was possible to pump on the lower bath with the transfer tube in place.

Electrical features

The electrical leads were #32 D.S.C. copper. The thermocouples and the leads entered the cryostat through a vacuum seal made by cementing them between a glass plate and a brass ring with Apiezon W. Together with the thermocouples, the lead wires were brought down the center pumping tube and were wound tightly around the stationary ring three times and the floating ring five times. The leads were wrapped around the adiabatic shield six times in a shallow groove machined in the cylindrical part of the shield for this purpose.

The sample heater was changed some from run to run, as explained below. For thorium and gadolinium the heater was of #38 constantan wire non-inductively wound in a helical groove machined in the heater shell. It had a resistance of approximately 130 ohms. Two #38 D.S.C. copper leads, which served as current leads, were soldered to the ends of the constantan heater close to the start of the helical winding. The #38 copper leads were wrapped 1½ times around the small heater ring, HR, and then taken to the outside of the adiabatic shield where they were soldered to the #32 copper leads. One potential lead was #38 copper and was joined to the current lead just as the current lead left the heater ring for the adiabatic shield. This potential lead was brought outside the adiabatic shield and soldered to a #32 copper lead. The second potential lead was a #32 copper lead connected to the second current lead where the latter last made contact with the adiabatic shield before going to the calorimeter proper.

For erbium the heater was non-inductively wound around the erbium sample itself and was lacquered to the erbium with G.E. #7031 adhesive. The heater was of #38 constantan and had a resistance of about 170 ohms. Two #38 copper leads were attached to the constantan heater ends. Three inches of these copper leads were inside the calorimeter can. The copper leads then came out of the can through a Stupakoff seal, were wound once around the bushing in which the Stupakoff was seated, and were taken to the #32 copper leads outside the adiabatic shield. A method similar to that used for gadolinium and thorium was used in connecting the potential leads. The connections were made where the current lead just came in contact with the outside of the calorimeter can for one potential lead, and just outside the adiabatic shield for the other.

In all cases, the two #38 current leads traversing the space between the shield and calorimeter were equivalent and the heat developed in each was, therefore, the same. On the assumption that the heat developed in the current leads divided equally between shield and calorimeter, the arrangement of leads correctly measured the heat supplied to the calorimeter.

The thermometer was a Leeds and Northrup 8164-A platinum resistance thermometer with a nominal resistance of 25.5 ohms at 0°C. It was calibrated by the National Bureau of Standards, and the temperature scale used was, therefore, the temperature scale of the National Bureau of Standards.[37,38]

The leads which emerged from the thermometer were made of platinum.

About $\frac{1}{2}$ inch from where they emerged from the glass, #40 nyltex-covered copper wires were soldered to them. These splices and the excess platinum wire were doubled back on the shank of the thermometer and were bound down with silk thread and G.E. adhesive. From the thermometer the #40 copper leads went to the heater ring and were wound around it $1\frac{1}{2}$ times. From this ring they were taken to the outside of the adiabatic shield and connected to the #32 copper lead wires.

As mentioned previously, the #32 copper leads for the thermometer, for the heater, and for the difference thermocouples, along with a number of spares (a total of 30 wires) were wound in a spiral groove on the side of the adiabatic shield. These wires were covered with one coat of corex before winding and two additional coats after winding. The wires were secured to the shield at the extremities by a thread strung through #60 holes on either side of the groove. The entire surface of the cylinder was then covered by #10 gold foil, followed by a layer of cigarette paper. G.E. adhesive was used both as a cement and as an aid in insulation. The heating element of the side of the shield was non-inductively wound on top of the cigarette paper. It was made of #30 constantan wire and had a resistance of 590 ohms. This heater was given three coats of G.E. adhesive and covered with #20 gold foil.

The top of the adiabatic shield was wound non-inductively with #38 D.S.C. constantan and had a resistance of 760 ohms. The bottom of the adiabatic shield was similarly wound and had a resistance of 745 ohms.

The floating ring was wound non-inductively with #35 D.S.C.

constantan wire having a resistance of 300 ohms and was covered with gold foil. Since the stationary ring was in direct thermal contact with the lower reservoir, it was not provided with a heater.

The direct thermocouples, which were used only for trouble-shooting, were made of #36 D.S.C. copper and #30 D.S.C. constantan wire. They were joined to the surfaces by soldering on the stationary ring, floating ring, the side, top and bottom of the adiabatic shield, and to the calorimeter proper. They were numbered from 5 to 10 and placed as shown in Figure 2.

There were four difference thermocouples between the following components: 1, block side-adiabatic shield side; 2, block bottom-shield bottom; 3, block top-shield top; and 4, floating ring-shield top. They were made of #35 D.S.C. constantan wire and #40 nyltex-covered copper wire for the thorium and gadolinium runs. Before the erbium run the difference thermocouples were changed in two ways: they were made longer so that more of the thermocouple could be lacquered down to come to equilibrium with its component part, and #38 D.S.C. copper was used instead of the smaller copper used previously.

The difference thermocouple junctions on the block were secured in rose-metal-filled wells of copper blocks which were bolted to the block. The junctions on the shield were held between pieces of mica under copper tabs and were secured with G.E. adhesive which provided both mechanical stability and thermal conductivity. At least six inches of each difference thermocouple ahead of the junction were lacquered to the inside of the adiabatic shield to assure thermal equilibrium. To assure thermal equilibrium between the block junctions and the block, all difference thermocouples were passed around a thermocouple ring, TR, (Figure 2) 2½ times before going to their block junction.

The ring-shield difference thermocouple was soldered to the ring at one end and lacquered in the bundle of leads where they first contact the adiabatic shield at the other end.

Electrical measuring circuits

At the experimental station there was a Bakelite barrier strip having pure copper terminals. All electrical leads from the experimental rig were soldered to these terminals, from which a permanent cable went to the main switchboard. The cable was a lead-shielded Western Electric 248 B.S. Interphone Cable containing 18 pairs of 22 gauge and 2 pairs of 18 gauge copper wires. The main switchboard was fabricated of 3/8 inch Bakelite sheet and contained five rows of copper D.P.D.T. knife switches, ten switches in a row. The first four switches on the top row plus all ten of the second row were used for the adiabatic calorimeter. All of the components of the thermometer and heater circuits except the potentiometers, their selector switches, and the timer were housed in the same cabinet as the main switchboard.

A White double potentiometer, which was generally used for heater and thermometer measurements, was located on the table next to the main switchboard. It had a range of 0-99990μv., with one unit on the last dial corresponding to 10μv. A twelve-position selector switch with silver contacts routed various e.m.f.'s to the White from the main switchboard. To improve sensitivity of adjustment in the upper and lower branches of the White, the arrangement shown in Figure 3 was put in series with each battery circuit.

The Wenner potentiometer, which was generally used to read the voltages of the direct thermocouples, was located on another table next to the White potentiometer table. It had two ranges: 0-0.111110 volts and 0-0.011111 volts. The desired range was obtained by setting the "x1, x0.1" switch on the potentiometer. The twelve-position selector switch for the Wenner was all copper. The sensitivity control for the Wenner and shield control circuit in Figure 4 was used along with the selector switch to apply any voltage from the main switchboard to the Wenner or directly to the galvanometer.

Each potentiometer had its own galvanometer, Leeds and Northrup Type 2285, having a sensitivity of approximately .0032μa./mm. at one meter. The galvanometer deflections were viewed through sixteen-power telescopes. The galvanometer mirrors reflected a 0-1000 mm. scale drawn on translucent tracing paper, which was illuminated from behind by fluorescent lights. The scales were approximately 6.5 meters from the galvanometers. Difference thermocouple 4 did not go through the Wenner selector switch, but went through an Ayrton Shunt and then to its own galvanometer, Type 2285. The deflection of this galvanometer was read on a ground glass scale at one meter distance from the galvanometer.

Figure 3

White current regulator circuit

Figure 4

Sensitivity control for Wenner and shield heater circuit

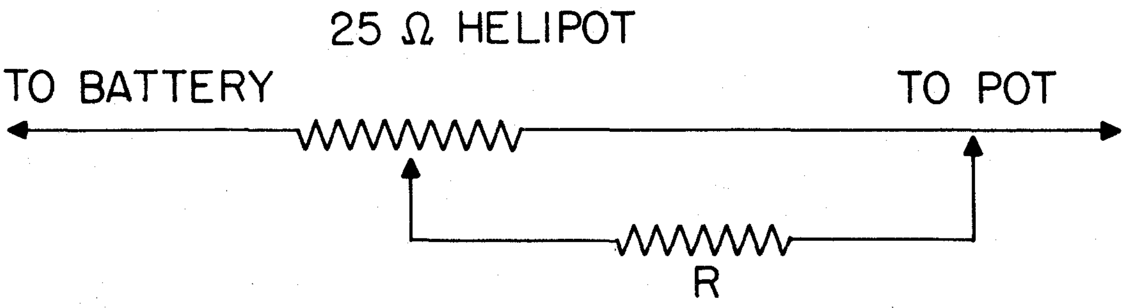
25 Ω HELIPOT
TO BATTERY
TO POT
R

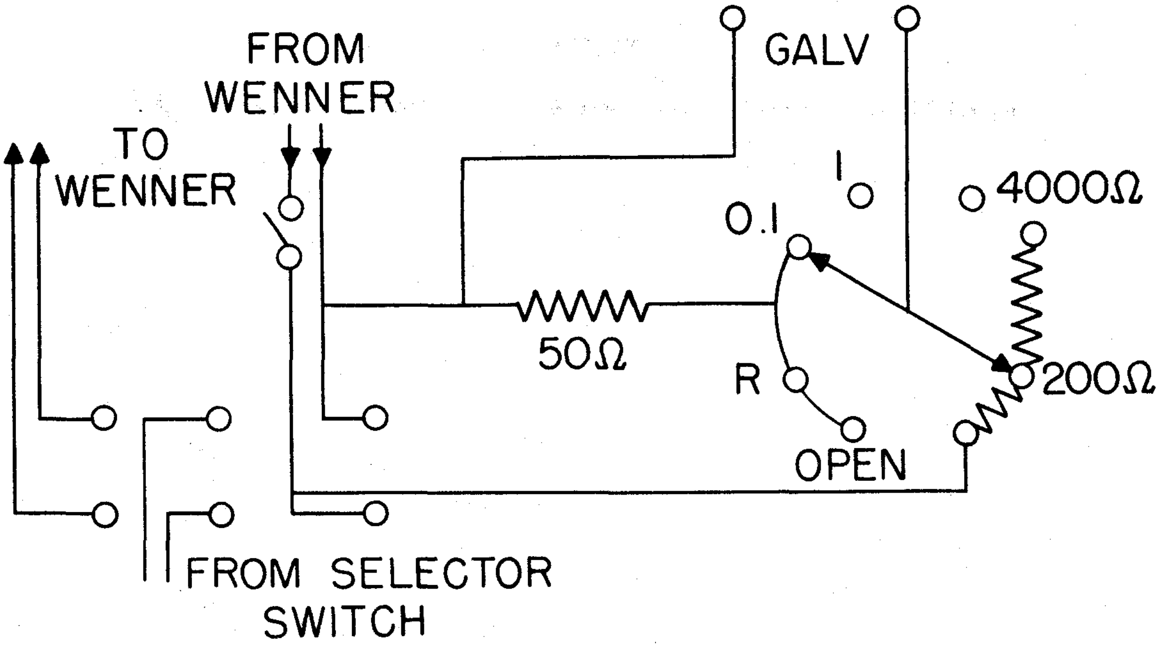
FROM WENNER
TO WENNER
GALV
I
0.I
4000Ω
50Ω
R
200Ω
OPEN
FROM SELECTOR SWITCH

Each potentiometer had its own set of Willard low-discharge batteries located in a central battery cabinet and also its own standard cell. The White had two Willard DH-5-1 batteries and the Wenner had two DD-5-3 batteries in parallel.

The thermometer circuit is shown in Figure 5. Current from a six-volt battery of three Willard DH-5-1 cells was sent through the platinum resistance thermometer via the I_R switch of the main switchboard. Measurement of I_R, the e.m.f. across either the 25 ohm or the 100 ohm standard resistor, permitted calculation of current through the thermometer. The 25 ohm resistor (switch A and switch B up) was used for a thermometer current of four ma. The 100 ohm resistor (switch A and switch B down) was used for thermometer currents of one ma. Switch C was kept closed if the 525 ohm and the 2100 ohm branches were desired in parallel. When switch D was closed, it short-circuited across the thermometer to allow exercise of the thermometer circuit without passing current through the thermometer.

The voltage across the thermometer was routed through the E_R switch to the potentiometer. Application of Ohm's law gave the thermometer resistance from E_R and I_R.

Electrical energy was furnished to the block heater from a battery of 15 Willard low-discharge cells, Type DD-5-1. By means of two 25 position, non-shorting, single-pole switches connected as shown in Figure 5, it was possible to obtain any desired current with either polarity. With the heater-exercise switch in heater position, the

Figure 5

Heater and thermometer circuits

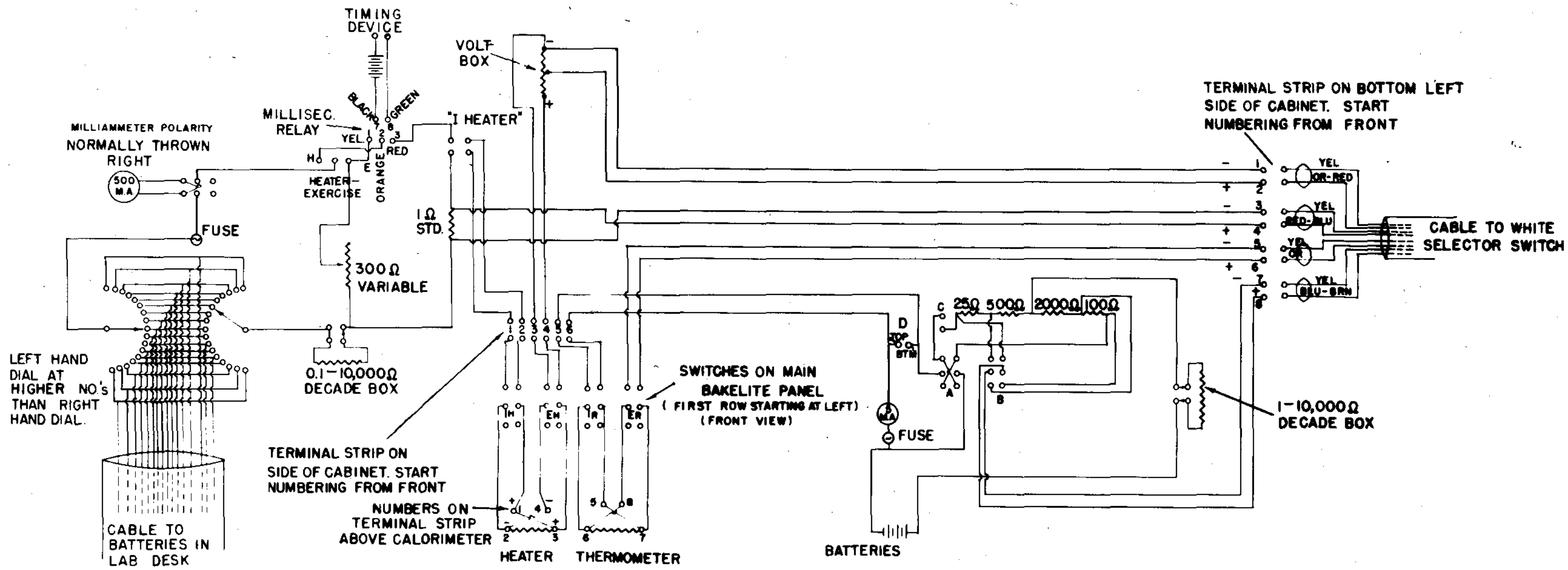
TIMING DEVICE
BLACK
GREEN
MILLISEC. RELAY
YEL.
RED
ORANGE
1
2
3
H
E
HEATER-EXERCISE
MILLIAMMETER POLARITY
NORMALLY THROWN RIGHT
500 M.A.
FUSE
VOLT BOX
"I HEATER"
1Ω STD.
300Ω VARIABLE
0.1-10,000Ω DECADE BOX
LEFT HAND DIAL AT HIGHER NO.'s THAN RIGHT HAND DIAL.
CABLE TO BATTERIES IN LAB DESK
TERMINAL STRIP ON SIDE OF CABINET. START NUMBERING FROM FRONT
1 2 3 4 5 6
I_H
E_H
I_R
E_R
NUMBERS ON TERMINAL STRIP ABOVE CALORIMETER
1 4 2 3 5 6 6 7
HEATER
THERMOMETER
SWITCHES ON MAIN BAKELITE PANEL
(FIRST ROW STARTING AT LEFT)
(FRONT VIEW)
D
TOP
BTM
MA
FUSE
BATTERIES
C
A
B
25Ω 500Ω 2000Ω 100Ω
1-10,000Ω DECADE BOX
TERMINAL STRIP ON BOTTOM LEFT SIDE OF CABINET. START NUMBERING FROM FRONT
− 1
+ 2
− 3
+ 4
− 5
+ 6
− 7
+ 8
YEL
OR-RED
YEL
RED-BLU
YEL
OR
YEL
BLU-BRN
CABLE TO WHITE SELECTOR SWITCH

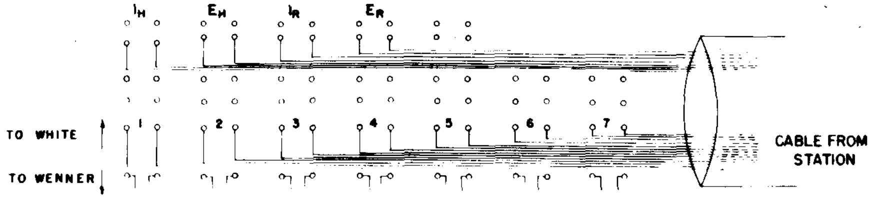
I_H
E_H
I_R
E_R
TO WHITE
TO WENNER
1 2 3 4 5 6 7
CABLE FROM STATION

current went through the Millisec Relay* to the heater via the I switch on the master switchboard and back to the battery through the one ohm standard resistor and the decade resistance box. If the Millisec Relay was not energized, or if the heater-exercise switch was thrown to the "exercise" position, the current was routed through a 300 ohm adjustable dummy heater, the decade resistance box, and back to the batteries. The current in the heater circuit, I, was calculated from the potential drop across the one ohm standard resistor. The voltage drop across the heater, E, was measured by means of a volt box. Knowledge of I and E enabled the calculation of power expended in the heater.

The heating interval for the sample was regulated by a Standard Electric Time Company pendulum clock in conjunction with a bench control unit of the same manufacturer. The Millisec Relay was energized by a six-volt battery of four #6 dry cells with the circuit being controlled by the bench unit of the clock. The bench control unit could be set as desired for any number of integral seconds up to 2500 seconds. Accuracy of the time measurement was ± .004 seconds as checked by oscillograms of the standard frequency of radio station WWV.

The adiabatic shield control unit, shown in Figure 6, was similar to that used by Scott, *et al.*[25] It was mounted on a Bakelite panel with the selector switch and sensitivity control for the Wenner and shield control circuit. The shield heating currents were routed through a lead-shielded cable to the barrier strip at the experimental station.

---

*This relay was Type 172, manufactured by Stevens-Arnold, Inc., South Boston, Mass.

Figure 6

Adiabatic shield control circuit

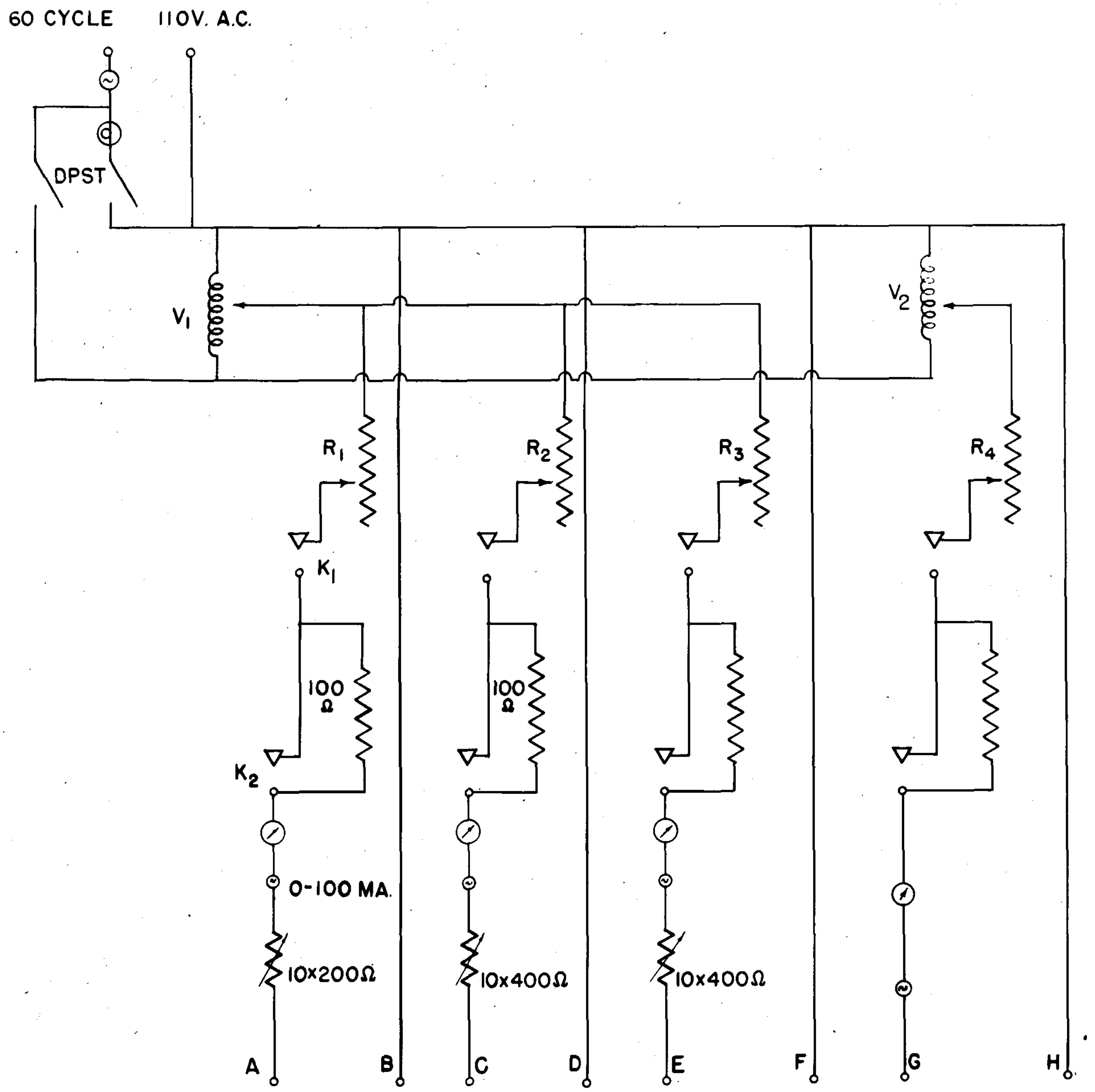

V

V_1 & V_2 1 AMP VARIAC TRANSFORMERS
K_1 NORMALLY CLOSED KEY SWITCHES
K_2 NORMALLY OPEN
R_1, R_2, R_3, R_4 500Ω 50W

EXPERIMENTAL PROCEDURE AND TREATMENT OF DATA

Experimental Procedure

General

The data necessary for the direct determination of an average value of heat capacity over a certain temperature interval are: measurement of the electric power introduced into the sample, the time interval during which the power is introduced, and the temperature change due to the power input. The measurement of a single heat capacity is here called a determination and a series of determinations is called a run.

The calorimeter can or block (henceforth, either assembly will be called block) was first cooled to the lowest temperature desired for that particular run by placing it in thermal contact with the cold reservoir, R_1, and its attached shield, S_1, by means of helium exchange gas. When the desired temperature was reached, the exchange gas was pumped out, leaving the block thermally isolated. A determination was then made by measuring the initial temperature of the block, putting a measured amount of electrical energy into the block, and then measuring the final temperature. During a run the final temperature of one determination was also the initial temperature of the next. The adiabatic shield was always kept at the same temperature as the block in order to eliminate heat exchange between the block and its surroundings.

The procedure outlined above was carried out over the entire range to determine the gross heat capacity of the sample plus all the auxiliary parts such as the thermometer, heater, calorimeter can, thermocouple tabs, etc. The sample was then removed from the calorimeter and the heat capacity of the auxiliary parts was determined. Subtraction of the heat capacity of the auxiliary parts from the gross heat capacity gave the heat capacity of the sample.

Two operators were required for the operation of the calorimeter; one made the temperature and power measurements while the other controlled the temperature of the shield and the floating ring.

Adiabatic shield control

In controlling the temperature of the adiabatic shield use was made of difference thermocouples 1, 2, 3, and 4 to measure temperature differences between the various parts of the block and shield and ring. (See Figure 2 for placement of these thermocouples.) Most generally the e.m.f.'s from 1, 2, and 3 were applied directly to the galvanometer by means of the switching arrangement shown in Figure 4. With the e.m.f.'s being applied directly to the galvanometer a sensitivity of about 8 cm./μv. was obtained, which corresponded roughly to 300 cm./deg. at room temperature. The e.m.f. from 4 was read on a ground glass scale of 1/6 the optical path of the others, and its sensitivity was, therefore, only 1/6 that of the others. In both cases, the galvanometer scales could be read to ± 0.3 mm.

The goal of adiabatic shield control was to maintain the readings of the difference thermocouples at zero. Since it was impossible to read the e.m.f.'s of all the difference thermocouples and control the heater currents simultaneously, some preference had to be given to the various ones. The area of the side of the block comprised 78 per cent of its total surface area so 1, which measured the difference in temperature between the shield side and the block side was always read first and followed most closely during large changes in temperature of the shield and block. The electrical leads between the shield and the block came out at the bottom of the shield so 2 was given second preference, with 3 being read last and followed least closely. A constant check of 4 could be made since it had a separate galvanometer.

The temperature of the various components of the shield and the ring was controlled by regulating the current in their respective heaters. The reservoir, R_1, and its shield, S_1, were required to have a temperature lower than the shield and block to provide a mechanism for cooling the shield. Experience was the greatest guide in judging how much to change the heater currents when the difference thermocouple readings were off-zero. When large changes of heater currents were required in all the shield and ring heaters, such as at the start or end of a block heating period, the variacs were used. (See Figure 6.) Large changes in the individual heater currents were produced by means of the decade resistors, while small individual changes were produced by adjusting the variable resistors. The key switches, K_2, were used for non-permanent increases in heater currents and the toggle switches, K_1, were used for non-permanent decreases. A record was kept of the settings of the variac, decade resistors, and variable resistors for each heater. This helped greatly when large changes of heater currents were needed at the beginning and end of block heating periods. The settings of the variacs, decade resistors, and variable resistors changed very little from one block heating period to the next and from one to the next interim period (that time between block heating periods when the temperature of the block was coming to equilibrium and when this temperature was being recorded by the operator at the White).

Below 200°K. it was generally possible to keep the temperature of various parts of the shield such that the difference thermocouples were within an average of ± 3 mm. of zero, which corresponded to ± .001°K. As the temperature increased from 200 to 300°K. the accuracy of control decreased to about an average of ± 8 mm., but due to increased sensitivity of the thermocouples this was still ± .002°K. The least accurate control was encountered at the beginning or the end of the block heating periods, when for short periods of time the control was worse than the figures stated above.

Since the temperature of the lower reservoir, R_1, and its shield, S_1, would presumably be a factor in the ease and accuracy of control of the adiabatic shield, various refrigerants were used in the lower reservoir during the thorium run to determine their effect upon the adiabatic shield control and accuracy of measurements. From 200 to 300°K. liquid nitrogen was used as the refrigerant for one run and pulverized solid carbon dioxide was used for another. A bath of ice water was used from

273 to 300°K. in a third run.

Below 273°K. the results of the measurements were in very good agreement for the runs using the different refrigerants. The temperature drift of the block due to imperfect adiabatic conditions was minute in both cases, but was a factor of 1.5 to 2 larger in the case of liquid nitrogen over the solid carbon dioxide bath. It was noted during the runs, however, that the pressure in the inner vacuum system remained lower at the highest temperatures in the runs when a liquid nitrogen bath was used. This fact, along with the greater ease in using liquid nitrogen, resulted in the choice of liquid nitrogen over solid carbon dioxide as a refrigerant in this range.

Between 273 and 300°K. the drift rates due to non-adiabatic conditions for the runs using an ice bath, solid carbon dioxide, and liquid nitrogen were in the respective ratio of 2:3:4. The absolute drift rates were approximately .0001°/min. to .0002°/min. in this range. Upon comparing heat capacities from these various runs, it was found that the runs using ice and liquid nitrogen for refrigerants agreed very well, while the run using solid carbon dioxide gave slightly lower results. A higher pressure in the inner vacuum system was noted when the solid carbon dioxide was used, which may be a reason for the slight disagreement in results. The choice of refrigerants in this range seemed to be either liquid nitrogen or ice. If a run would have to be interrupted to change refrigerants, it would be better to use liquid nitrogen up to 300°K. Otherwise, the use of ice would be as good a choice due to its economy and ease of preparation.

Some trouble was encountered in the adiabatic shield control during the measurements on gadolinium which was attributed to thermal gradients existing on the surface of the block during block heating periods. Extensive investigations of the temperature distribution on the block and on the shield were made along with measurements of the heat leakage modulus between the block and adiabatic shield. These investigations were carried out at liquid nitrogen, solid carbon dioxide, ice and room temperatures. The result of the above investigations indicated that by proper control of the temperature of all components of the adiabatic shield the error from the non-adiabatic conditions was .01 to .02 per cent at maximum, which was negligible.

Temperature and power measurements

As previously explained, the temperature and power measurements were taken alternately during a run. The data necessary for temperature determination were E_R, the voltage drop across the thermometer, and I_R, the voltage drop across the standard resistor in series with the thermometer. The quantities E_R and I_R were measured alternately during a determination at time intervals of either one or two minutes. In most cases, the time required for the block to reach thermal equilibrium after a heating was less than ten minutes, in which case the intervals between readings were one minute. When a period longer than ten minutes was required for thermal equilibrium to be established in the block, two minute intervals between E_R and I_R readings were generally used.

The procedure for taking an E_R or I_R reading was: the dials of the White were set as closely as possible to the incoming e.m.f., the unbalance e.m.f. from the White was read on the galvanometer, the control knob on the White was turned to "check" and the resultant galvanometer reading was noted. The results of all three steps were recorded at the time they were obtained.

The "check" position on the White serves two purposes. First, it substitutes for the external circuit a neutral resistor of equal value in order to keep the galvanometer sensitivity constant, and second, it routes the battery current through dummy resistors rather than through the potentiometer dials. The dummy resistors have the same resistance as the potentiometer dials so there is no change in battery voltage during the time when the "check" reading is made. When the control knob is on "check", the galvanometer reads its mechanical zero plus any spurious e.m.f.'s in the instrument or galvanometer circuit. This "check" reading was used instead of the galvanometer mechanical zero because it automatically compensated for the spurious e.m.f.'s in the instrument and galvanometer.

In order that the galvanometer reading in cm. could be converted into an e.m.f., a determination of the galvanometer sensitivity in μv./cm. had to be made. This was done by reading the galvanometer deflection for one setting of the White, changing the White by 10 μv. and noting the galvanometer deflection, and finally noting the galvanometer deflection after changing the White back to its original setting. The galvanometer deflection for the original setting was linearly interpolated to the time when the reading for the 10 μv. change was taken. The difference between the two galvanometer readings at this time was the sensitivity in cm./10 μv. The sensitivity was different for the various circuits external to the White and changed during the run for each circuit so a sensitivity measurement was made for each measured quantity about every sixth determination.

Since both the resistance of the thermometer and its dR/dT (change of resistance with temperature) became smaller at lower temperatures, the thermometer current was increased from 1 ma. to 4 ma. for determinations below 50 or 60°K. This increase in current caused an increase in the voltage drop across the thermometer and, therefore, improved the accuracy of temperature measurement. The higher thermometer current was not used at higher temperatures because the power dissipation in the thermometer became inconveniently large as the thermometer resistance increased.

The data necessary for power calculation were E, the voltage drop across a fraction of the volt box in parallel with the heater, and I, the voltage drop across a resistor in series with the heater. Readings of E and I were taken alternately at 1 minute intervals during the block heating period. The procedure for measuring E and I was similar to that used for E_R and I_R. Sensitivities were taken in the same manner and with about the same frequency as for E_R and I_R readings.

The measurement of the time of the block heating period consisted of setting the dials on the bench control unit of the clock circuit for the desired time interval and turning on the timer. Turning on the timer started the heating current and after the desired number of seconds had elapsed, the timer and heating current were automatically shut off.

Factors entering into the choice of a block heating current were a convenient length for the heating period and a desirable ΔT (final temperature minus initial temperature of a determination). The minimum time in which reliable measurements of the power could be made was 300 seconds. The maximum time of a heating period was 900 seconds and this seemed inconveniently long. The optimum length of the heating period was from 400 to 600 seconds. For normal behavior of the heat capacity the ΔT's were approximately 10 per cent of the absolute temperature up to 40°K. and they were from 3.5 to 4.5 degrees between 40 and 300°K. When abnormalities in the heat capacity were encountered, the ΔT's were decreased. Since larger temperature intervals were more convenient, some determinations were made using ΔT's of six to seven degrees, and these gave excellent agreement with other values.

Volt box settings were made such that the E reading would be in the range from 70,000 to 90,000 μv. for the largest currents in the run.

Treatment of Data

Temperature

The first step in the treatment of the thermometer data was to calculate the correct voltage of each E_R and I_R reading by the following formulae:

$$E_R = E_{Dials} + \frac{\text{galvanometer - check}}{\text{sensitivity (cm./10}\mu\text{v.)}} \tag{1}$$

$$I_R = I_{Dials} + \frac{\text{galvanometer - check}}{\text{sensitivity (cm./10}\mu\text{v.)}} \tag{2}$$

where E_{Dials} and I_{Dials} = White dial settings for E_R and I_R

galvanometer = deflection of galvanometer due to unbalance voltage of White

check = check reading for that particular E_R or I_R reading

sensitivity = the galvanometer sensitivity determined for the respective quantities being measured

Since the E_R and I_R were determined at different times, plus the fact that they were not constant, it was necessary to interpolate the values of I_R readings to the time when the E_R readings were taken. The I_R readings were interpolated because (due to circuit design) they changed more slowly than the E_R readings. The resistance of the thermometer at the time of each E_R reading was then calculated from the relation:

$$R_T = (E_R/I_R)\, R_S \tag{3}$$

where R_T = resistance of the thermometer

R_S = resistance of the standard in series with the thermometer

For most determinations there was a small temperature drift of block temperature even after thermal equilibrium had been established. This was caused by inability to obtain perfect adiabatic conditions and, in some cases, by heating due to thermometer current. When the change in resistance of the thermometer per unit time had become constant after a heating period, this constant change or drift was considered to be due to non-adiabatic conditions.

Calculation of the final temperature of a determination was made in the following manner: the resistance of the thermometer was chosen at a time when the drift had become constant, the drift was assumed to be the same between the middle of the heating period and the chosen time, the drift/minute multiplied by the time between the middle of the heating period and the chosen time was subtracted from the resistance at the chosen time to give the "corrected" resistance of the final temperature, the temperature corresponding to the "corrected" final resistance was calculated from a temperature versus resistance table.

The initial temperature of a determination was calculated in the same manner as the final temperature with the corrections for the drift being made from a chosen initial time to the middle of the heating period and added to the resistance at the chosen initial time. For each determination the temperature increase, ΔT, was obtained from the relation:

$$\Delta T = T_f - T_i \tag{4}$$

where T_f = final temperature of the determination

T_i = initial temperature of the determination

The temperature versus resistance table referred to above was prepared from tables and constants supplied for this thermometer by the National Bureau of Standards. The resistance was given for each 0.1° between 10 and 90°K. and for each 1.0° between 90 and 375°K. The maximum error due to linear interpolation over these intervals was supposed to be ± .001°K.

Heat input

The first step in calculation of power was to calculate the correct voltage for each E and I reading by using relations similar to (1) and (2). The E readings were more stable than the I readings so the E readings were interpolated to the time of the I readings. The power, W, was then calculated at the time of the I reading by the relation:

$$W = (I/R_1 - E/R_2)\ (E \times R_3/R_2) \tag{5}$$

where E = voltage drop across a fraction of the volt box

I = voltage drop across a 1 ohm standard

R_1 = resistance of the 1 ohm standard

R_2 = resistance of that part of the volt box across which E was measured

R_3 = total resistance of volt box and leads in parallel with the heater

The term E/R_2 is a correction for the current which goes through the volt box instead of through the heater.

Extensive investigations were made during the Gd experiment on the best way to calculate the average power of a determination from values of the power at various times during that determination. The results of these investigations showed that the maximum error in the calculation of an average power, if it were assumed to be changing linearly during the heating period, would be .003 per cent. In almost all of the cases examined, the error was less than .0001 per cent. The power at the mid-point of the heating period was, therefore, used as the average power for that determination.

The heat input, ΔQ, for the heating period was found by the relation:

$$\Delta Q = W_{ave.} \times t \quad \text{joules} \tag{6}$$

where $W_{ave.}$ = power in watts at the mid-point of the heating period

t = time of power input in seconds

Heat capacity calculations

The mean gross heat capacity, C_g, for each determination on the block plus auxiliary parts was calculated from the relation:

$$C_g = \frac{\Delta Q}{T \times 4.1840} \quad \text{cal./deg.} \tag{7}$$

The factor 4.1840 in the denominator was necessary to convert joules (watts x seconds) into thermochemical calories.

For each determination, the mean heat capacity of the auxiliary parts was found by relation (9). These values were plotted and a smooth curve was drawn through the points. From this curve it was possible to obtain the mean heat capacity of the auxiliary parts corresponding to each temperature of the mean gross heat capacity measurements. The heat capacity of the sample was then calculated from the relation:

$$C_{p-m} = \frac{C_g - C_{aux.}}{n} \text{ cal. deg.}^{-1} \text{ (g. atom)}^{-1} \tag{8}$$

where C_{p-m} = mean heat capacity of the sample over the temperature range of C_g

$C_{aux.}$ = heat capacity of auxiliary parts at mean temperature of C_g

n = number of moles of sample

The value of C_{p-m} could be thought of as the value of $[C_p]_{T_m}$ (the actual heat capacity at the mean temperature of the determination) if C_p were assumed to vary linearly with temperature. A formula developed by Osborne and co-workers[51] corrects the value of C_{p-m} to $[C_p]_{T_m}$. This formula is:

$$[C_p]_{T_m} = C_{p-m} - \left(\frac{\partial^2 C_p}{\partial T^2}\right)_{T_m} \frac{\Delta T^2}{24} - \left(\frac{\partial^4 C_p}{\partial T^4}\right)_{T_m} \frac{\Delta T^4}{1924} - \cdots \tag{9}$$

where $[C_p]_{T_m}$ = true value of heat capacity at mean temperature of determination

$T_m = \frac{T_f + T_i}{2}$, or mean temperature of determination in which T_f and T_i were final and initial temperatures

Approximations of $\left(\frac{\partial^2 C_p}{\partial T^2}\right)_{T_m}$ were obtained by evaluating $\left(\frac{\Delta^2 C_{p-m}}{\Delta T^2}\right)_{T_m}$ from the experimental values of C_{p-m}. The value of $\left(\frac{\Delta^4 C_{p-m}}{\Delta T^4}\right)_{T_m}$ was negligible in all cases.

The corrections for the values of C_{p-m} to give $[C_p]_{T_m}$ for thorium were negligible above 30°K. and amounted to, at most, 0.3 per cent below 30°K. For gadolinium the corrections to three values near the peak of the anomaly amounted to about one per cent, four more values had 0.1 to 1 per cent corrections, and the rest had negligible corrections. Corrections to some of the erbium values below 20°K. amounted to two per cent.

There were no corrections to values around the 55°K. anomaly and corrections to only three values at the 84°K. anomaly greater than 0.1 per cent. In general, the absence of these corrections was due mainly to the small ΔT's used in ranges of rapidly changing heat capacity.

In the cases of thorium and gadolinium, the heat capacity of the sample plus the heater, thermometer, and other auxiliary parts was first measured. A thin copper shell was then substituted for the sample in an otherwise identical set-up, and the heat capacity of the copper shell plus the auxiliary parts was determined. The difference in heat capacity of the two runs plus the heat capacity of the copper shell was the net heat capacity of the sample. The heat capacity of the weighed copper shell was well known from work of Giauque and Meads,[26] which was confirmed by measurements in this laboratory.

A similar but somewhat more complicated procedure was followed in the case of erbium, since it was contained in a can and the heater was wound around the sample. In this case, an exact duplicate of the heater was wound around a thin-walled hollow copper cylinder which was substituted for the erbium sample. The heat capacity of the can plus copper dummy was determined. These values, corrected for the known heat capacity of the copper dummy, were subtracted from the values of the initial runs to give the net heat capacity of erbium.

In each case, a plot of the final C_p values versus temperature was made and the best curve drawn through these points. The smoothed values of C_p presented in the tables and used for calculating the thermodynamic functions were taken from this curve.

Values of C_V at room temperature were obtained from the thermodynamic relationship:

$$C_p - C_V = TV\alpha^2/\beta \tag{10}$$

where T = temperature of the calculation

V = volume per gram atom

α = coefficient of cubical expansion $= \frac{1}{V}\left(\frac{\partial V}{\partial T}\right)_p$

β = volume compressibility $= \frac{-1}{V}\left(\frac{\partial V}{\partial p}\right)_T$

Values of $C_p - C_V$ at temperatures where α or β were not known could be found from the empirical relationship due to Nernst and Lindemann[27]:

$$C_p - C_V = A\, C_p^2\, T \tag{11}$$

where A is a constant.

Thermodynamic functions

The following relations define the thermodynamic functions at any temperature:

$$S^\circ - S^\circ_0 = \int_0^T C_p/T\, dT \tag{12}$$

where we have assumed in all cases that $S^\circ_0 = 0$.

$$H^\circ - H^\circ_0 = \int_0^T C_p dT \tag{13}$$

$$\frac{F^\circ - H^\circ_0}{T} = \frac{H^\circ - H^\circ_0}{T} - S \tag{14}$$

The actual evaluation of the above integrals was accomplished with the aid of Simpson's "1/3 rule" of numerical integration. The temperature intervals used for the numerical integrations varied from 0.1 to 5.0°K.

depending on how rapidly the heat capacity was changing over the temperature range to be integrated.

The Debye function was used in extrapolation of the data from the lowest determined values of C_p to 0°K. The value of the Debye θ_D or characteristic temperature was found from the lowest temperature measurements of C_p (which was equal to C_v at those temperatures) by use of θ_D/T versus C_v tables.[28] The average value of θ_D found for the lowest four or five determinations was then used to obtain values of C_p on down to 0°K. from the same tables.

RESULTS

Thorium

The experimental values of C_p, before correction by equation (9), and ΔT for thorium are listed in Table 2 in the order they were measured. The values of C_p in Table 3 were taken from a smooth curve drawn through the corrected values of C_p. A graph of C_p versus T is shown in Figure 7. The values of C_v in Table 3 were calculated by means of equation (10) and equation (11). The density at 25°C. was taken to be 11.61[29] corresponding to $V = 19.99$ cc./g. atom. The value of β, 16.48×10^{-13} cm.^{2}/dyne, was computed from measurements by Reynolds[30] of Young's modulus and Poisson's ratio. This value was chosen instead of the direct experimental result of Bridgman,[31] 18.55×10^{-13} cm.^{2}/dyne, since the material used by Reynolds was made at the Ames Laboratory while Bridgman's measurements were made when thorium was not obtainable in as high a purity as presently. The thermal expansion coefficient was taken as 32.58×10^{-6} deg.$^{-1}$ from the work of Erfling.[32] The value of $C_p - C_v$ obtained at 25°C. was 0.092 cal. deg.$^{-1}$ (g. atom)$^{-1}$. The constant A in equation (11) for calculation of $C_p - C_v$ at other temperatures was $7.20_4 \times 10^{-6}$ (g. atom) cal.$^{-1}$.

The extrapolation of C_p below 18°K. was accomplished by means of the Debye equation with a value of $\theta_D = 141.6$. This value of θ_D was the average value of those values calculated from experimental points in the

Table 2

Experimental values of C_p for thorium, cal. deg.$^{-1}$ (g. atom)$^{-1}$

Atomic weight = 232.12 0°C. = 273.16°K.

Mean T (°K.)	Approx. ΔT	C_p	Mean T (°K.)	Approx. ΔT	C_p
	Run 1				
79.51	3.87	5.123	194.53	3.96	6.198
83.35	3.80	5.217	198.50	3.95	6.213
87.13	3.74	5.295	202.44	3.94	6.226
90.85	3.70	5.358	206.37	3.93	6.242
94.52	3.66	5.409	210.50	4.33	6.261
98.16	3.62	5.461	214.82	4.31	6.276
101.77	3.59	5.506	219.83	4.30	6.290
105.34	3.56	5.555	223.42	4.28	6.315
108.89	3.53	5.596	227.69	4.27	6.327
112.40	3.50	5.638	235.05	4.24	6.352
115.89	3.48	5.674	239.29	4.24	6.359
119.35	3.45	5.717	243.52	4.23	6.369
122.79	3.43	5.748	247.74	4.21	6.388
126.22	3.41	5.780	251.94	4.20	6.399
129.62	3.39	5.813	256.14	4.19	6.413
134.17	4.23	5.847	260.33	4.18	6.425
138.39	4.20	5.880	264.50	4.17	6.438
142.58	4.18	5.914	268.66	4.16	6.454
146.74	4.16	5.939	272.82	4.15	6.459
150.89	4.13	5.972	276.95	4.13	6.483
154.18	4.12	5.990	281.08	4.12	6.496
158.29	4.10	6.021	285.20	4.12	6.499
162.38	4.08	6.041	289.30	4.10	6.523
166.45	4.06	6.062	293.40	4.09	6.530
170.51	4.05	6.087	297.48	4.07	6.556
174.55	4.03	6.102			
178.57	4.02	6.127			
182.58	4.00	6.143			
186.58	3.99	6.162			
190.56	3.98	6.181			

Table 2 (Continued)

Mean T (°K.)	Approx. ΔT	C_p
	Run 2	
58.42	3.78	4.451
61.89	3.65	4.608
65.48	3.54	4.738
68.99	3.46	4.845
72.41	3.39	4.939
75.773	3.33	5.027
79.075	3.27	5.109
82.323	3.22	5.191
	Run 3	
57.70	4.04	4.420
61.66	3.88	4.599
65.48	3.76	4.739
69.19	3.67	4.864
72.83	3.59	4.954
76.39	3.53	5.046
79.99	3.46	5.136
80.74	4.06	5.155
84.76	3.99	5.245
88.72	3.93	5.322
92.63	3.88	5.383
96.49	3.84	5.437
100.31	3.80	5.489
104.09	3.76	5.535
107.84	3.73	5.583
111.55	3.70	5.627
115.24	3.67	5.667
122.91	3.62	5.774
126.51	3.59	5.783
130.09	3.57	5.817
133.66	3.55	5.846
137.20	3.53	5.867
140.73	3.52	5.885
144.24	3.49	5.946
147.72	3.48	5.951
151.20	3.46	5.992
154.65	3.45	5.998
158.10	3.44	6.016
161.92	4.20	6.045
166.12	4.19	6.062
170.30	4.17	6.085
174.47	4.16	6.105
178.61	4.14	6.125
182.75	4.12	6.147
186.81	4.59	6.162
191.39	4.57	6.184
195.95	4.55	6.204
200.49	4.53	6.228
205.02	4.52	6.239
209.53	4.51	6.252
214.04	4.52	6.232
218.53	4.47	6.289
223.00	4.46	6.307
227.45	4.44	6.327
231.89	4.44	6.335
236.32	4.42	6.348
240.73	4.41	6.367
245.13	4.40	6.378
249.52	4.38	6.399
253.90	4.37	6.413

Table 2 (Continued)

Mean T (°K.)	Approx. ΔT	C_p	Mean T (°K.)	Approx. ΔT	C_p
258.63	4.36	6.418		Run 5	
262.45	4.02	6.382			
266.64	4.36	6.418	138.79	3.02	5.887
270.97	4.31	6.488	141.87	3.13	5.678
275.28	4.32	6.466	144.93	3.00	5.927
			147.92	2.99	5.954
279.59	4.31	6.477	150.90	2.97	5.981
283.89	4.30	6.492	153.88	2.96	5.995
288.18	4.29	6.498	156.84	2.95	6.012
292.45	4.28	6.510			
296.71	4.27	6.522			
				Run 6	
	Run 4		275.43	4.27	6.471
			279.69	4.26	6.487
16.15	1.88	0.694	283.95	4.25	6.497
18.97	1.75	0.984	288.19	4.24	6.503
21.39	1.92	1.255	292.42	4.23	6.519
23.57	2.11	1.593	296.64	4.22	6.531
25.83	2.36	1.906			
28.37	2.72	2.215			
31.11	2.77	2.504			
34.05	3.11	2.815			
37.22	3.23	3.120			
40.44	3.19	3.392			
43.58	3.09	3.629			
47.06	3.85	3.866			
51.10	4.24	4.107			
55.24	4.03	4.322			
59.19	3.87	4.501			

Table 3

Heat capacity of thorium, cal. deg.$^{-1}$ (g. atom)$^{-1}$

Atomic weight = 232.12 0°C. = 273.16°K.

T°K.	C_p	C_v	T°K.	C_p	C_v
20	1.106	1.106	170	6.083	6.039
25	1.801	1.800	175	6.109	6.062
30	2.397	2.396	180	6.133	6.084
35	2.910	2.899	185	6.155	6.105
40	3.355	3.352	190	6.177	6.125
45	3.733	3.728	195	6.197	6.143
50	4.048	4.042	200	6.217	6.161
55	4.309	4.302	205	6.237	6.180
60	4.529	4.520	210	6.256	6.197
65	4.723	4.713	215	6.275	6.214
70	4.878	4.866	220	6.293	6.230
75	5.011	4.997	225	6.310	6.245
80	5.132	5.117	230	6.330	6.264
85	5.248	5.231	235	6.347	6.279
90	5.342	5.323	240	6.362	6.292
95	5.415	5.395	245	6.379	6.307
100	5.482	5.460	250	6.392	6.318
105	5.547	5.524	255	6.407	6.332
110	5.607	5.582	260	6.422	6.345
115	5.664	5.637	265	6.437	6.358
120	5.717	5.689	270	6.453	6.372
125	5.767	5.737	275	6.468	6.385
130	5.815	5.783	280	6.483	6.398
135	5.857	5.824	285	6.497	6.410
140	5.895	5.860	290	6.510	6.421
145	5.931	5.894	295	6.524	6.434
150	5.965	5.894	298.16	6.532	6.441
155	5.996	5.956	300	6.538	6.446
160	6.026	5.984			
165	6.055	6.011			

Figure 7

Heat capacity of thorium

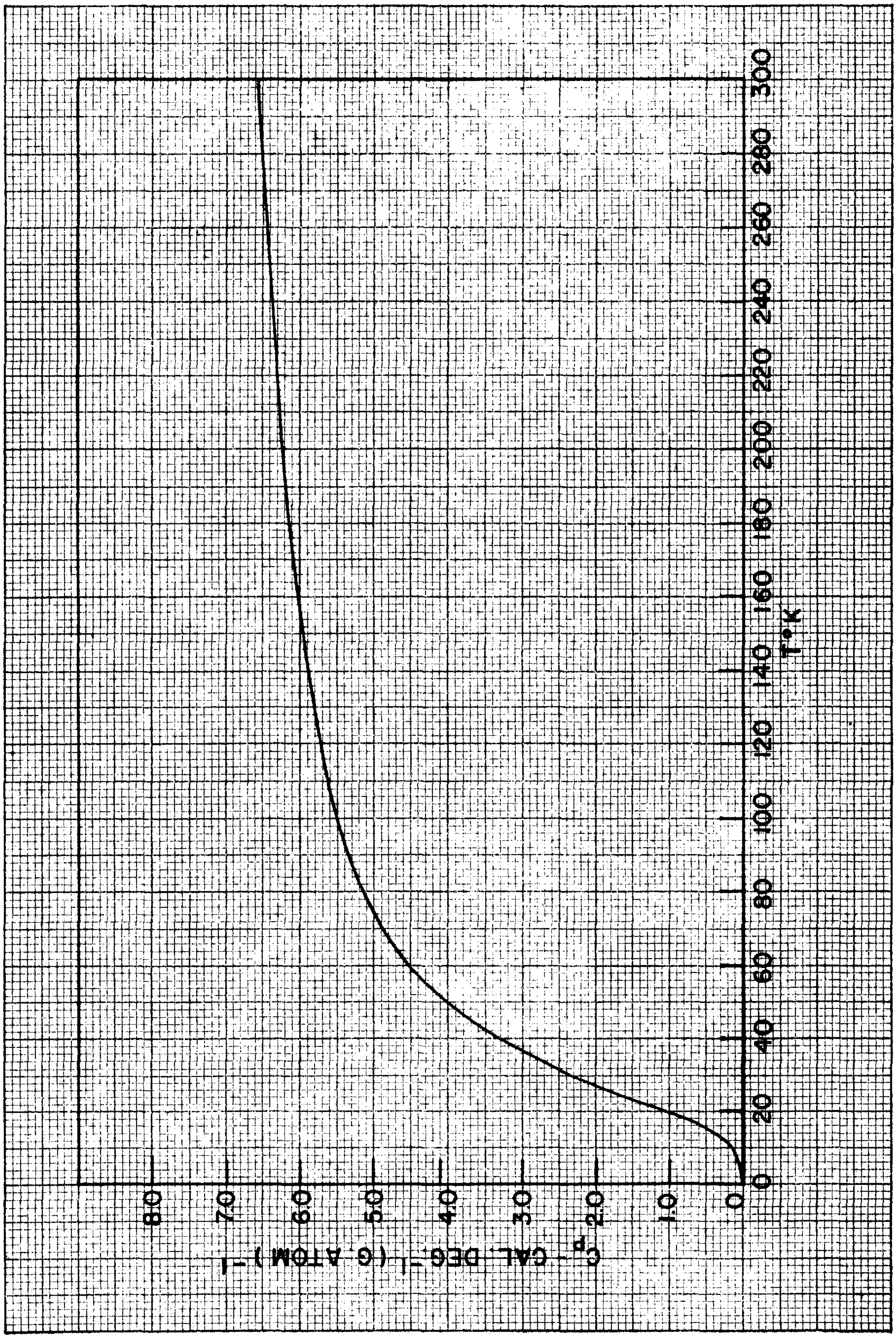
C_p - CAL. DEG.$^{-1}$ (G. ATOM)$^{-1}$
0
1.0
2.0
3.0
4.0
5.0
6.0
7.0
8.0
T°K
0
20
40
60
80
100
120
140
160
180
200
220
240
260
280
300

temperature range from 18-28°K. The electronic heat capacity was assumed to give a negligible contribution to the C_p values in this range.

In Table 4 the thermodynamic functions, as calculated by evaluation of equations (12), (13), and (14), are listed. The values of C_p used for the integrations were taken from the smooth curve.

Table 4

Thermodynamic functions of thorium

Cal. deg.$^{-1}$ (g. atom)$^{-1}$

T°K.	S^o	$\frac{H^o - H^o_0}{T}$	$\frac{-(F^o - H^o_0)}{T}$
20	0.410	0.304	0.106
50	2.770	1.801	0.969
100	6.135	3.369	2.766
150	8.460	4.164	4.296
200	10.215	4.648	5.567
250	11.623	4.980	6.643
298.16	12.760	5.220	7.540
300	12.799	5.228	7.571

The precision of the measurements can best be expressed by the deviation of the experimental values of C_p from a smooth curve drawn through these values. Below 20°K. the deviation ranged from 0 to ± 2 per cent. Between 20-135°K. all but three points lay well within ± 0.1 per cent of the curve and these three were within ± 0.2 per cent. Between 135-155°K. the largest scatter of points was obtained with several points deviating ± 0.3 per cent. From 155-300°K. the deviations were all within 0.1 per cent except for three points within ± 0.2 per cent around 300°K. At least 70 per cent of the points over the entire range lay right on the curve.

The drift corrections due to imperfect adiabatic conditions were never larger than 0.1 per cent of the total ΔT for any determination between 20-300°K. Below 20°K. some of the drifts got very large, with the resulting corrections amounting to 10 or 20 per cent of the total ΔT. Inability to maintain the bath at a temperature lower than that of the adiabatic shield was the reason for the large drifts below 20°K.

The heat capacity of the auxiliary parts amounted to one per cent of the total heat capacity at 20°K. This ratio increased with increasing temperature to a maximum of four per cent at room temperature.

The absolute accuracy of the measurements was governed by the ability to measure the temperature and temperature differences. The error in the measurement of temperature differences of about two degrees was thought to be at most ± 0.1 per cent above 30°K. Below 30°K. the error increased to approximately ± one per cent at 15°K. The accuracy of absolute temperature measurement was thought to have an error of ± 0.001°K. from room temperature down to about 30°K. which increased to ± 0.02°K. at 15°K. Heat capacity values obtained from the smooth curve were thought to be accurate to ± 0.1 per cent down to 30°K. and to ± 1 or 2 per cent at 15°K.

Gadolinium

The experimental values of C_p and ΔT for all of the gadolinium determinations are given in Table 5. The values of C_p in Table 6 were taken from a smooth curve drawn through the experimental values of C_p which had been corrected by equation (9) for non-linearity. Figure 8 shows a plot of this smooth curve.

Extrapolation of C_p from 15-0°K. was accomplished by using a value of $\theta_D = 152$ in the Debye equation. In obtaining the value of θ_D, an attempt was made to separate the lattice and the electronic heat capacities in the lowest measurements. At a sufficiently low temperature the lattice heat capacity can be assumed to vary as T^3, and the lattice plus electronic heat capacity can be represented as $C_v \approx C_p = \gamma T + AT^3$. A plot of C_p/T versus T^2 then permits the calculation of the coefficient γ. Application of this method to the lowest temperature results of gadolinium gave values of γ which were certainly too high, so it was assumed that the temperature of the results was not low enough to justify the T^3 lattice heat capacity assumption. The best method of approximation, therefore, seemed to be to assume the value of γ for gadolinium was the same as for lanthanum,[3] namely 16×10^{-4}. After sub-

Table 5

Experimental values of C_p for gadolinium, cal. deg.$^{-1}$ (g. atom)$^{-1}$

Atomic weight = 156.9 $\qquad$ 0°C. = 273.16°K.

Mean T (K.)	Approx. ΔT.	C_p
	Run 1	
58.57	4.52	5.268
62.97	4.29	5.542
67.16	4.10	5.792
71.19	3.97	5.963
75.10	3.85	6.135
78.90	3.75	6.286
82.59	3.65	6.431
86.21	3.57	6.559
89.75	3.51	6.664
93.24	3.46	6.754
96.67	3.41	6.835
100.52	4.29	6.928
104.78	4.22	7.025
108.97	4.16	7.111
113.10	4.10	7.194
117.18	4.05	7.278
121.21	4.00	7.347
125.19	3.96	7.413
128.69	3.92	7.475
132.59	3.88	7.539
136.46	3.85	7.601
140.28	3.81	7.656
144.08	3.78	7.725
147.84	3.74	7.786
151.57	3.71	7.831
155.69	4.51	7.897
160.18	4.46	7.974
164.62	4.42	8.047
169.01	4.37	8.122
173.36	4.33	8.189
177.67	4.29	8.258
181.94	4.25	8.324
186.18	4.21	8.394
190.36	4.17	8.466
194.51	4.13	8.538
198.62	4.09	8.613
202.69	4.05	8.693
206.72	4.01	8.781
210.87	4.58	8.856
215.42	4.52	8.953
219.91	4.47	9.048
224.35	4.41	9.164
228.74	4.35	9.265
233.08	4.30	9.380
237.36	4.23	9.512
241.57	4.18	9.640
245.74	4.12	9.759
249.83	4.04	9.945
253.87	3.97	10.108
257.84	3.90	10.299
266.31	3.73	10.748
273.60	3.56	11.251
279.62	3.39	11.775
282.95	3.28	12.296
285.41	1.66	12.516
287.05	1.63	12.791
288.65	1.58	13.148
290.21	1.54	13.565
291.75	1.56	13.383
293.54	2.05	10.048

Table 5 (Continued)

Mean T (K.)	Approx. ΔT	C_p	Mean T (K.)	Approx. ΔT	C_p
295.67	2.23	9.216		Run 3	
297.93	2.31	8.878			
300.26	2.37	8.637	274.43	2.21	11.284
302.64	2.42	8.457	276.44	1.81	11.474
305.02	2.46	8.296	278.42	2.14	11.637
			280.54	2.11	11.858
307.49	2.49	8.177	282.68	2.18	12.119
309.97	2.51	8.103			
312.49	2.54	8.001	284.61	1.68	12.384
315.03	2.56	7.944	286.27	1.65	12.635
317.59	2.59	7.827	287.61	1.08	12.873
			288.70	1.06	13.121
			289.74	1.04	13.410
	Run 2				
			290.66	0.82	13.681
15.10	3.59	0.467	291.47	0.80	13.850
18.00	2.22	0.754	292.30	0.87	12.782
19.96	1.69	0.989	293.28	1.08	10.229
21.51	1.41	1.189	294.39	1.15	9.586
23.45	2.47	1.453			
			295.85	1.78	9.211
26.05	2.73	1.814	297.95	2.46	8.881
28.66	2.49	2.177	300.43	2.53	8.627
31.30	2.79	2.537	303.90	4.83	8.368
34.28	3.16	2.944	308.78	4.95	8.132
37.31	2.91	3.326			
			313.75	5.04	7.970
40.19	2.85	3.654	318.80	5.12	7.834
45.10	3.45	4.175	323.90	5.18	7.731
48.43	3.20	4.488	329.05	5.22	7.666
51.54	3.02	4.752	334.24	5.26	7.600
54.48	2.87	4.979	339.47	5.31	7.512
62.89	6.44	5.542	344.74	5.37	7.421
				Run 4	
			337.33	5.15	7.482
			342.43	5.17	7.454
			347.54	5.21	7.378
			352.70	5.24	7.323
			357.82	5.26	7.287

Table 6

Heat capacity of gadolinium in cal. deg.$^{-1}$ (g. atom)$^{-1}$

Atomic weight = 156.9 0°C. = 273.16°K.

T°K.	C_p	T°K.	C_p	T°K.	C_p
15.0	0.456	140	7.655	265	10.673
20	0.995	145	7.734	270	10.979
25	1.664	150	7.813	275	11.349
30	2.363	155	7.893	280	11.802
35	3.035	160	7.973	285	12.446
40	3.632	165	8.054	290	13.468
45	4.160	170	8.135	295	9.402
50	4.627	175	8.215	300	8.667
55	5.012	180	8.293	305	8.316
60	5.361	185	8.374	310	8.086
65	5.670	190	8.458	315	7.926
70	5.922	195	8.547	320	7.805
75	6.134	200	8.641	325	7.715
80	6.337	205	8.738	330	7.650
85	6.520	210	8.842	335	7.586
90	6.670	215	8.944	340	7.499
95	6.796	220	9.051	345	7.415
100	6.914	225	9.170	350	7.350
105	7.026	230	9.299	355	7.309
110	7.134	235	9.440		
115	7.235	240	9.592		
120	7.329	245	9.757		
125	7.417	250	9.953		
130	7.499	255	10.168		
135	7.577	260	10.408		

Figure 8

Heat capacity of gadolinium

Form E-5

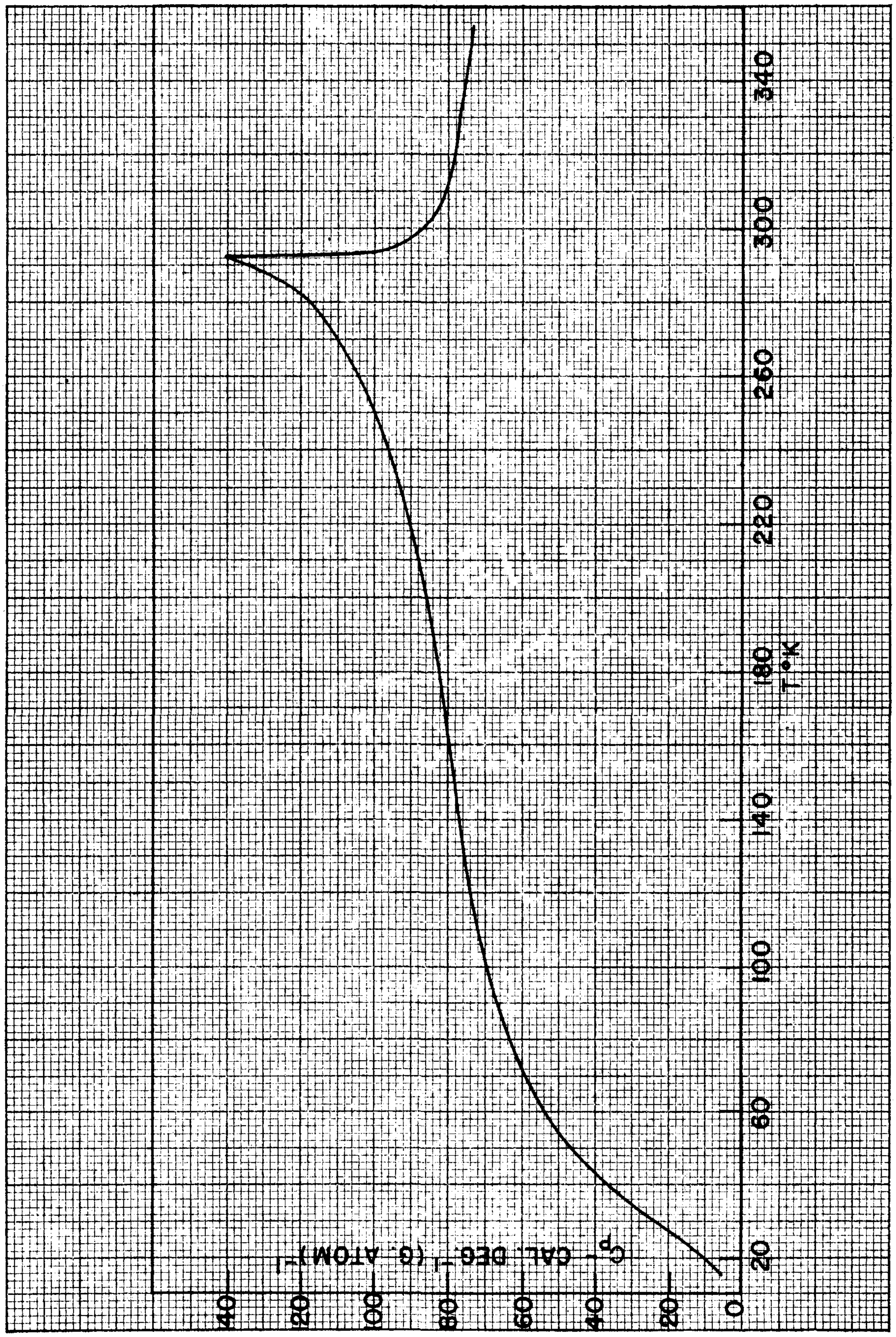
C_p - CAL. DEG.$^{-1}$ (G. ATOM)$^{-1}$
0
20
40
60
80
100
120
140
T°K
20
60
100
140
180
220
260
300
340

traction of the electronic contribution from each of the three lowest determinations, values of $\theta_D = 152$, 150, and 148 were obtained. The value of $\theta_D = 152$ was chosen. This value of θ_D is lower than the value obtained from a preliminary investigation of sound velocities in some of the rare earth metals.[33] The values obtained from the sound velocity measurements were lanthanum 162, gadolinium 176, dysprosium 180, and erbium 190. It is well known that values of θ_D obtained by various methods do not necessarily agree, so the difference in the θ_D for gadolinium obtained by the two methods is not alarming. Since the θ_D values were of interest mainly to predict thermal properties, the use of the values obtained from thermal measurement rather than from sound velocities seemed logical. The approximately linear increase in θ_D with atomic number noted in the sound velocity measurements would seem to justify the assumption, which will be used later, that the thermally determined values of θ_D also increase linearly with atomic number.

The thermodynamic functions in Table 7 were calculated using values of heat capacity taken from the smooth curve and equations (12), (13), and (14).

The calculation of $C_p - C_v$ entailed the following data. The isothermal compressibility, β, was determined by Bridgman[34] to be 25×10^{-7} cm.^{2}/kg. at room temperature. The coefficient of volume expansion, α, could be inferred from the work of Trombe and Foex,[15] which indicated that from -140 to 20°C. the linear expansion coefficient is zero. Their measurements indicated that α becomes positive and

Table 7

Thermodynamic functions of gadolinium

Cal. deg.$^{-1}$ (g. atom)$^{-1}$

T°K.	S°	$\frac{H^\circ - H^\circ_0}{T}$	$\frac{-(F^\circ - H^\circ_0)}{T}$
15	0.155	0.116	0.039
50	2.797	1.875	0.922
100	6.880	3.948	2.932
150	9.867	5.098	4.769
200	11.770	5.878	5.892
250	13.820	6.545	7.275
293	15.610	7.246	8.354
298.16	15.774	7.284	8.490
300	15.828	7.293	8.535
360	17.238	7.364	9.874

appreciable below -140°C., but they gave no quantitative figure. Above 20°C. they gave $\alpha = 8.3 \times 10^{-6}$ deg.$^{-1}$, which is comparable to the other rare earth metals. Measurements by Banister, Legvold, and Spedding[18] on the temperature variation of the lattice parameters of gadolinium were used to estimate a value of $\alpha = 1 \times 10^{-6}$ deg.$^{-1}$. Measurements made by Barson, Legvold, and Spedding[14] on a rolled sample of gadolinium gave values of α ranging from 6.4×10^{-6} deg.$^{-1}$ at 25°C. to 8.0×10^{-6} deg.$^{-1}$ at -170°C. The results of Trombe and Foex were used because of the approximate nature of the value of Banister, Legvold, and Spedding and because of the questionable rolled sample of Barson, Legvold, and Spedding. The density of 7.948, as determined by Klemm and Bommer,[35] along with a molecular weight of 156.9, gave an atomic volume of 19.74 cc./g. atom. The value of $C_p - C_v$ calculated at 25°C. was 0.034 cal. deg.$^{-1}$ (g. atom)$^{-1}$. Since the value of α was zero below 20°C., the value of $C_p - C_v$ also became zero below 20°C. Above 25°C. the value of $C_p - C_v$ would vary approximately by the factor T/298.

The precision of the measurements, as expressed by the deviation of the experimental points from a smooth curve, was as follows: below 60°K. all points were well within ± 0.1 per cent of the curve, with at least 95 per cent of the points within ± 0.05 per cent; between 60-200°K. all points were within ± 0.1 per cent with about 85 per cent of them within ± 0.05 per cent; between 200-355°K. all the points were within - 0.2 per cent with 90 per cent of them within ± 0.1 per cent of the curve. Since the precision stated above was for all points, it can be inferred that the various runs agreed within these limits.

The drift corrections due to non-adiabatic conditions ranged from one per cent of the total ΔT at 15°K. to zero at 20°K. Between 20-200°K. they were almost all zero and between 200-300°K. they ranged from 0.1 to 0.2 per cent of the ΔT. They increased above room temperature to about one per cent of the total ΔT at 355°K. The ratio of the heat capacity of the auxiliary parts to the total heat capacity ranged from one per cent at 15°K. to three per cent at 300°K.

The absolute accuracy of the measurements was governed by the ability to measure the temperature and the ΔT's. The error in these measurements is the same as stated for the thorium measurements. Heat capacity values obtained from the smooth curve were thought to be accurate to ± 0.1 per cent down to 30°K. and to ± 1 or 2 per cent at 15°K.

Erbium

The experimental values of C_p and ΔT are given for erbium in Table 8. These values are not corrected for non-linearity of C_p. A smooth curve was drawn through the values corrected by equation (9) and the values from this curve are given in Table 9. Values from this curve were used for the calculation of the thermodynamic functions given in Table 10. In those cases where the heat capacity was non-reproducible, the maximum value of the heat capacity at any given temperature was used in the calculation of thermodynamic properties.

Values of C_p between 15-0°K. were calculated using a value of $\theta_D = 89.0$ in the Debye heat capacity equation. This value was obtained from experimental values of C_p between 15.2-17.5°K. These temperatures were too high to allow determination of the electronic heat capacity, so this contribution was assumed to be the same as for lanthanum,[3] namely 0.0016 T cal. deg.$^{-1}$ (g. atom)$^{-1}$. After correction for the electronic contribution the experimental values of C_p gave values of θ_D ranging from 89.8 at 15.2°K. to 87.4 at 17.5°K. The chosen value of 89.0 was

Table 8

Experimental values of C_p for erbium, cal. deg.$^{-1}$ (g. atom)$^{-1}$

Atomic weight = 167.28 0°C. = 273.16°K.

Mean T (°K.)	Approx. ΔT	C_p
	Run 1	
59.62	3.26	6.884
62.83	3.17	7.032
65.96	3.01	7.179
69.01	3.01	7.310
72.01	2.95	7.428
74.93	2.89	7.547
77.79	2.83	7.674
80.59	2.77	7.805
83.33	2.71	7.978
86.30	3.22	6.453
89.63	3.45	5.893
93.07	3.43	5.878
96.49	3.41	5.880
98.90	3.39	5.883
102.27	3.35	5.921
105.61	3.34	5.910
108.93	3.31	5.943
112.23	3.28	5.970
115.50	3.26	5.995
119.23	4.22	6.015
123.43	4.19	6.048
127.59	4.14	6.080
131.71	4.11	6.099
135.81	4.08	6.123
139.87	4.05	6.147
143.91	4.02	6.173
147.92	4.00	6.196
152.27	3.97	6.222
156.23	3.96	6.225
160.18	3.94	6.245
164.10	3.92	6.254
168.02	3.91	6.261
171.91	3.88	6.304
175.77	3.85	6.336
179.61	3.83	6.370
183.43	3.81	6.390
187.67	4.80	6.416
192.44	4.78	6.439
197.20	4.76	6.454
201.94	4.74	6.469
206.66	4.72	6.491
211.35	4.70	6.495
216.04	4.69	6.511
220.70	4.67	6.521
227.87	4.63	6.539
232.49	4.62	6.542
237.08	4.60	6.559
241.66	4.59	6.572
246.23	4.58	6.579
250.78	4.56	6.597
255.31	4.55	6.607
259.84	4.54	6.606
264.34	4.52	6.629
268.83	4.51	6.648
273.30	4.50	6.645
277.77	4.48	6.673
282.03	4.10	6.675
286.27	4.46	6.687
290.69	4.45	6.702
295.09	4.44	6.715
299.49	4.43	6.724

Table 8 (Continued)

Mean T (°K.)	Approx. ΔT	C_p
	Run 2	
60.82	2.36	6.944
63.57	3.14	7.069
66.66	3.06	7.209
69.68	2.99	7.312
72.38	2.40	7.442
74.84	2.51	7.573
77.06	1.94	7.639
78.82	1.59	7.724
80.26	1.31	7.782
81.44	1.04	7.863
82.47	1.03	7.926
83.49	1.02	8.001
84.50	1.02	7.978
85.60	1.17	6.744
86.82	1.28	6.010
88.11	1.30	5.921
89.41	1.30	5.892
90.87	1.62	5.886
92.65	1.94	5.877
94.59	1.93	5.877
96.51	1.93	5.877
	Run 3	
142.55	4.00	6.159
146.53	3.97	6.183
150.49	3.95	6.210
154.43	3.93	6.227
158.34	3.91	6.240
162.23	3.89	6.262
166.11	3.87	6.280
169.97	3.85	6.306
173.81	3.83	6.329
177.62	3.81	6.361
	Run 4	
83.27	0.16	7.990
83.47	0.16	8.008
83.58	0.16	8.006
83.74	0.16	8.006
83.90	0.16	8.007
84.05	0.16	8.007
84.21	0.16	8.008
84.37	0.16	8.007
84.52	0.16	8.006
84.68	0.16	8.005
84.84	0.16	7.887
85.00	0.16	7.719
85.16	0.17	7.450
85.33	0.17	7.109
85.51	0.18	6.751
	Run 5	
297.12	4.75	6.713
301.86	4.74	6.721
306.59	4.73	6.730
311.29	4.72	6.743
315.98	4.71	6.757
320.66	4.70	6.758
325.32	4.69	6.771

Table 8 (Continued)

Mean T (°K.)	Approx. ΔT	C_p
	Run 6	
18.84	0.58	2.745
19.67	0.73	3.239
20.75	1.45	3.405
22.53	2.12	3.403
24.57	1.96	3.664
26.98	2.86	4.134
29.69	2.58	4.564
32.49	3.00	4.853
35.38	2.78	5.201
38.33	3.11	5.548
41.34	2.91	5.887
44.28	2.98	6.207
47.19	2.82	6.505
50.27	3.35	6.803
53.63	3.26	6.953
56.98	3.26	6.869
60.08	3.21	6.916
	Run 7	
15.21	0.38	1.647
15.79	0.78	1.796
16.93	1.51	2.095
18.48	1.58	3.020
20.01	1.54	4.658
22.01	2.47	3.590
	Run 8	
18.90	0.64	2.967
19.65	0.87	3.955
20.54	0.95	3.604
21.59	1.15	3.691
23.00	1.47	3.454
24.56	1.64	3.662
26.50	2.24	4.015
28.62	2.01	4.470
	Run 9	
17.75	1.41	2.334
19.23	1.56	3.181
20.71	1.40	3.519
22.13	1.45	3.389
23.76	1.80	3.548
25.49	1.67	3.809
	Run 10	
24.19	1.80	3.544
26.29	2.41	3.967
50.07	1.91	6.787
52.19	2.33	6.940
54.46	2.31	6.935
56.82	2.32	6.853
59.13	2.30	6.883
61.41	2.26	6.974
63.65	2.22	7.072
	Run 11	
54.81	1.36	6.770
56.15	1.34	6.786
57.48	1.32	6.824
58.80	1.31	6.859
60.10	1.30	6.911
61.40	1.29	6.966

Table 8 (Continued)

Mean T (°K.)	Approx. ΔT	C_p
	Run 12	
53.35	1.38	6.735
54.72	1.37	6.783
56.08	1.35	6.826
57.44	1.35	6.816
58.78	1.34	6.863
60.11	1.32	6.922
61.42	1.31	6.970
62.72	1.29	7.034
	Run 13	
16.01	0.98	1.859
17.03	1.08	2.118
18.09	1.07	2.550
19.04	0.87	3.763
19.93	0.95	4.300
20.94	1.29	3.801
22.27	1.40	3.461
23.65	1.37	3.538
24.98	1.29	3.730
27.16	3.09	4.168
30.42	3.43	4.642
34.01	3.76	5.039
37.61	3.44	5.464
41.34	4.03	5.885
45.22	3.73	6.301
48.01	1.86	6.622
49.84	1.80	6.762
51.61	1.76	6.904
53.36	1.73	6.972
55.09	1.74	6.916
56.83	1.74	6.853
58.57	1.73	6.865
60.29	1.71	6.923
	Run 14	
47.36	2.88	6.369
49.71	1.82	6.693
51.50	1.76	6.883
53.25	1.74	6.952
54.99	1.74	6.906
56.73	1.74	6.849
58.47	1.73	6.860
	Run 15	
16.79	0.76	2.062
17.60	0.86	2.268
18.46	0.86	2.724
19.16	0.53	3.725
19.77	0.71	4.363
20.46	0.67	3.741
21.15	0.72	3.433
21.87	0.73	3.393
22.60	0.72	3.407
23.48	1.05	3.500
24.51	1.01	3.649
	Run 16	
20.39	0.86	2.934
21.23	0.81	3.041
22.02	0.76	3.234
22.94	1.08	3.416
24.00	1.03	3.570

Table 8 (Continued)

Mean T (°K.)	Approx. ΔT	C_p
	Run 17	
18.34	0.50	2.896
18.88	0.57	3.313
19.44	0.56	4.452
19.92	0.42	4.977
20.34	0.35	4.770
20.70	0.39	4.261
21.22	0.67	3.815
21.99	0.89	3.545
22.98	1.08	3.519
24.04	1.05	3.608
25.06	1.01	3.751

Table 9

Heat capacity of erbium, cal. deg.$^{-1}$ (g. atom)$^{-1}$

Atomic weight = 167.28 0°C. = 273.16°K.

T°K.	C_p	T°K.	C_p	T°K.	C_p
5	0.082[a]	130	6.088	255	6.605
10	0.623[a]	135	6.120	260	6.618
15	1.600	140	6.148	265	6.634
20	5.020	145	6.178	270	6.648
25	3.733	150	6.207	275	6.660
30	4.602	155	6.231	280	6.673
35	5.515	160	6.253	285	6.687
40	5.737	165	6.277	290	6.701
45	6.278	170	6.306	295	6.710
50	6.778	175	6.338	298.16	6.716
55	6.918	180	6.371	300	6.718
60	6.911	185	6.399	305	6.729
65	7.136	190	6.422	310	6.742
70	7.348	195	6.442	315	6.752
75	7.550	200	6.461	320	6.757
80	7.775	205	6.480		
85	7.710	210	6.494		
90	5.889	215	6.507		
95	5.877	220	6.520		
100	5.884	225	6.534		
105	5.903	230	6.546		
110	5.948	235	6.557		
115	5.988	240	6.567		
120	6.022	245	6.579		
125	6.055	250	6.591		

[a] These values were obtained from the Debye extrapolation between 0°K. and 15°K.

Table 10

Thermodynamic functions of erbium

Cal. deg.$^{-1}$ (g. atom)$^{-1}$

T°K.	S°	$\frac{H^\circ - H^\circ_0}{T}$	$\frac{-(F^\circ - H^\circ_0)}{T}$
15	0.647	0.475	0.172
24	2.093	1.491	0.602
52	6.150	3.627	2.523
60	7.137	4.063	3.074
70	8.234	4.502	3.732
84.6	9.686	5.048	4.638
88	9.944	5.105	4.839
100	10.696	5.198	5.498
150	13.144	5.482	7.662
200	14.963	5.692	9.271
250	16.420	5.860	10.560
298.16	17.594	5.989	11.605
300	17.634	5.993	11.641
320	18.069	6.039	12.030

chosen for two reasons: it would provide a continuous curve at 15°K.; and although it would admittedly give values much too large for lattice heat capacity only, it would be better than the higher value of θ_D to approximate the total heat capacity below 15°K.

The smooth curve values of C_p were plotted to give Figure 9. Figure 10 shows the results of several runs through the temperature range of the 20°K. anomaly, displaying the "hysteresis" effects at these temperatures. The history of the sample for the various runs was as follows:

Run 6. The block was cooled from room temperature to 17.3°K. and the run was started. This was the first time that the block had been cooled below 55°K.

Run 7. After run 6 had gone from 17.30 to 61.68°K., the block was cooled to 15.02°K. and this run was started.

Run 8. The block was cooled from room temperature down to about 17.5°K. when the reservoir ran out of liquid hydrogen. The block warmed up to about 25°K. before it was cooled back to 18.58°K. and this run was started.

Run 9. After run 8 had been carried to 29.62°K., the block was cooled to 17.04°K. and this run was started.

Run 13. The block was cooled from room temperature to 15.52°K. and this run was started.

Run 15. An attempt was made to use liquid helium as a refrigerant to cool below 20°K. The supply of liquid helium was exhausted at around 18°K. and the temperature of the block got back to

Figure 9

Heat capacity of erbium

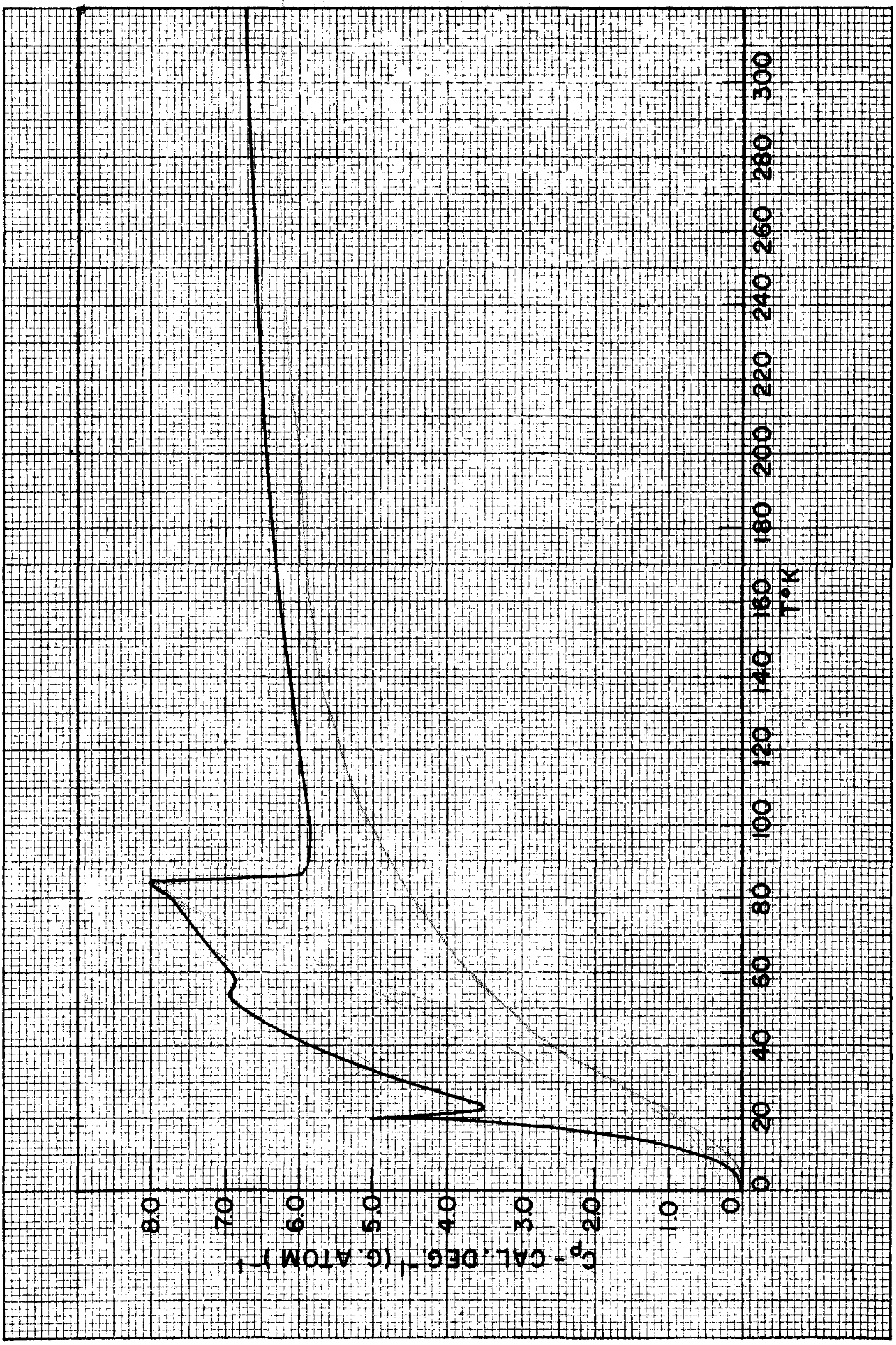
0
20
40
60
80
100
120
140
160
180
200
220
240
260
280
300
T°K
0
1.0
2.0
3.0
4.0
5.0
6.0
7.0
8.0
C_p - CAL. DEG.$^{-1}$(G. ATOM)$^{-1}$

Figure 10

Heat capacity of erbium in the region around 20°K.

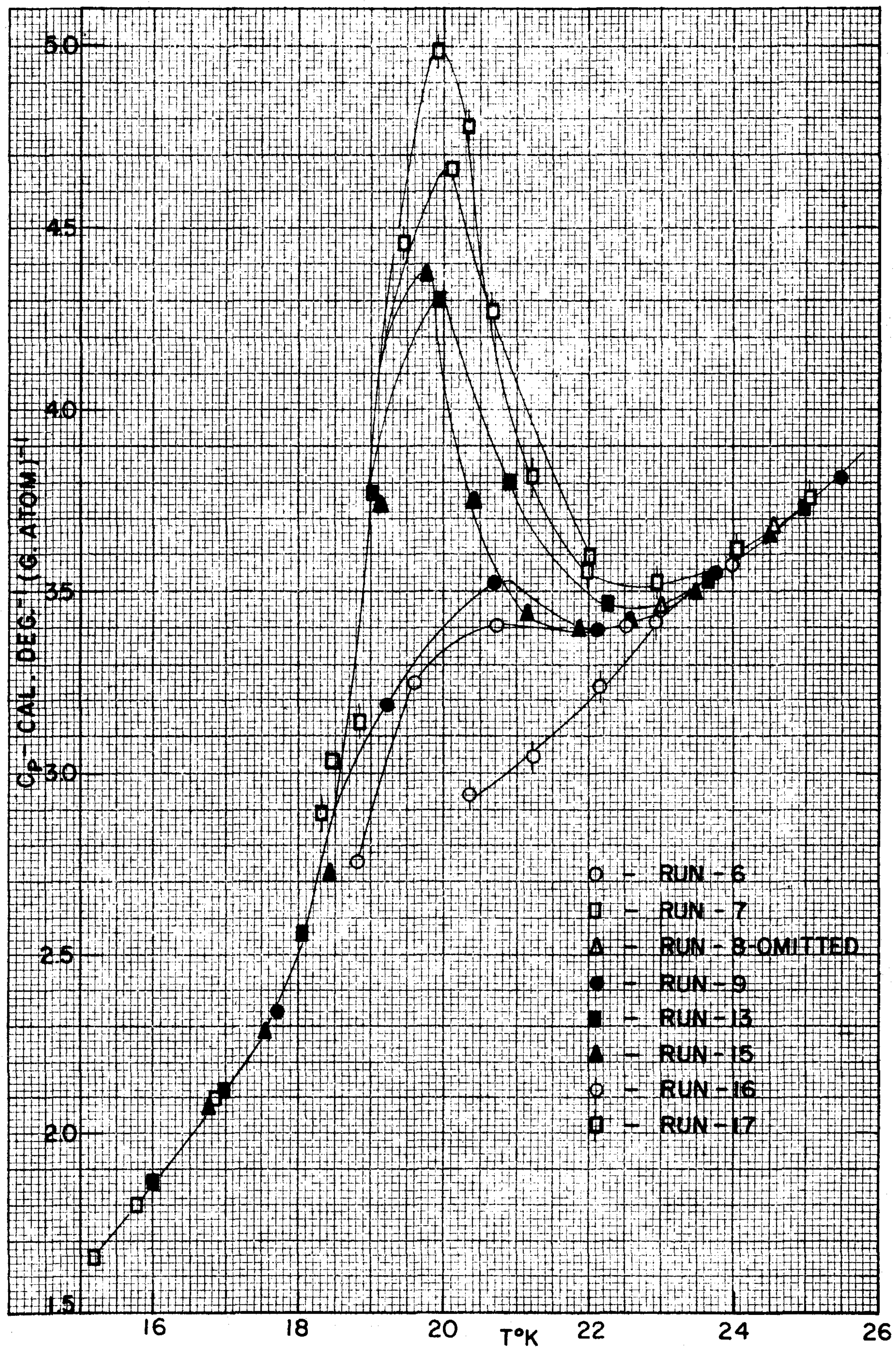
5.0
4.5
4.0
3.5
3.0
2.5
2.0
1.5
C_p - CAL. DEG.^-1 (G. ATOM)^-1
16
18
20
T°K
22
24
26
○ - RUN - 6
□ - RUN - 7
△ - RUN - 8 OMITTED
● - RUN - 9
■ - RUN - 13
▲ - RUN - 15
○ - RUN - 16
□ - RUN - 17

28°K. before it was cooled to 16.41°K. and this run was started. Cooling for this run started from room temperature.

Run 16. After run 15 had been carried to 25.01°K., the block was cooled to 19.96°K. and this run was started.

Run 17. The block was cooled from room temperature to 20°K. with liquid nitrogen and liquid hydrogen. Liquid helium was used to further cool the block to 10°K. before the supply was exhausted. The exchange gas was then pumped out, liquid hydrogen put in the lower reservoir and it was pumped on. Meanwhile, the temperature of the block had risen from 10 to 18.09°K. This run was then started.

Figure 11 shows the results of several runs through the temperature range of the 53°K. anomaly, displaying the "hysteresis" effect in this region. The history of the block for these various runs was as follows:

Run 6. The block was cooled from room temperature to 17.31°K. and measurements were started at this temperature.

Run 10. After run 9 the block was allowed to cool overnight to 23.39°K. Two determinations were made in this region and the block was heated to 49.11°K. where the rest of the run was started.

Run 11. The block was cooled to 54.13°K. from room temperature and this run was started.

Run 12. The block was cooled from room temperature to 52.66°K. and this run was started.

Figure 11

Heat capacity of erbium in the region around 53°K.

Form E-5

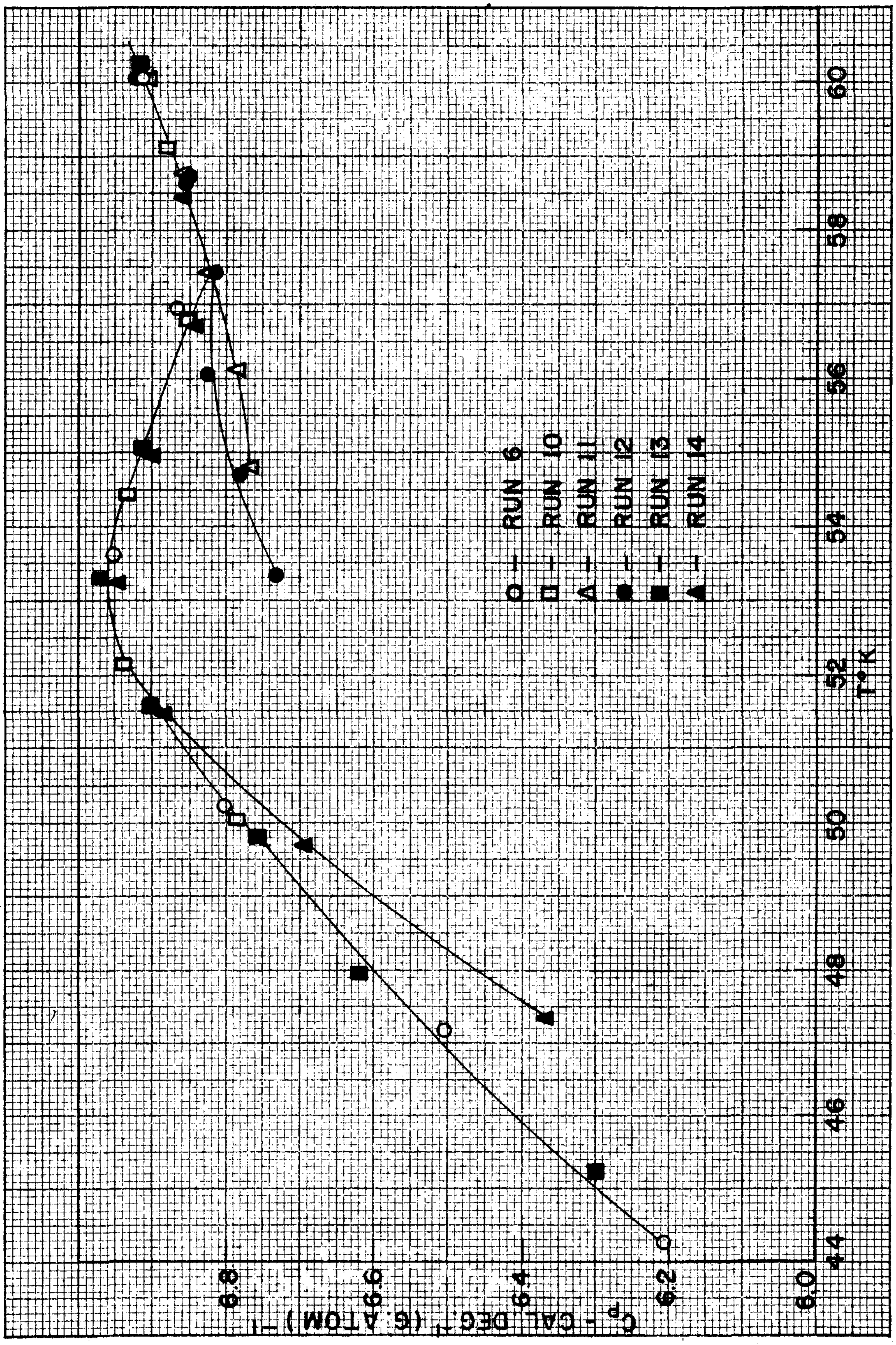
○ — RUN 6
□ — RUN 10
△ — RUN 11
● — RUN 12
■ — RUN 13
▲ — RUN 14
44
46
48
50
52
54
56
58
60
T°K
6.0
6.2
6.4
6.6
6.8
C_p - CAL DEG.$^{-1}$ (G ATOM)$^{-1}$

Run 13. The block was cooled from room temperature to 15.51°K. and this run was started.

Run 14. After run 13 had gone to 61.14°K., the block was cooled to 45.92°K. and this run was started.

The following data were used for the calculation of $C_p - C_v$ by equation (10). The volume compressibility was determined by Bridgman[36] to be 2.46×10^{-6} cm.^{2}/kg. Direct measurement of the linear expansion coefficient of erbium from room temperature to 100°K. by Barson, Legvold, and Spedding[14] gave 8.9×10^{-6} deg.$^{-1}$ at room temperature and slightly smaller values at lower temperatures. X-ray measurements of the temperature variation of the lattice parameters of erbium were used by Banister, Legvold, and Spedding[18] to obtain the approximate value of 12×10^{-6} deg.$^{-1}$ for the linear expansion coefficient from 100-300°K. Below 100°K. the value was approximately zero. These same measurements were also used to calculate a value of 9.020 for the room temperature density of erbium. From the values $\alpha = 26.7 \times 10^{-6}$ deg.$^{-1}$, $\beta = 2.46 \times 10^{-6}$ cm.^{2}/kg., $V = 18.55$ cm.^{3}/g. atom, and $T = 298.16$, the value of $C_p - C_v$ at 25°K. = 0.037 cal. deg.$^{-1}$ (g. atom)$^{-1}$ was obtained.

With the exception of a few isolated cases, the values of C_p between 15-300°K. did not deviate from the smooth curve by more than 0.1 per cent and in approximately 85 per cent of the cases they were within 0.05 per cent. Above 300°K. some deviations from the smooth curve amounted to ± 0.3 per cent with an average of about ± 0.1 per cent. The drift corrections for a single determination were a maximum of two per cent of the ΔT below 20°K., from 0 to 0.2 per cent between 20-50°K., from

0 to 0.3 per cent between 50-200°K., and from 0.3 to 1 per cent from 200-300°K. The ratio of heat capacity of can to total heat capacity was 1/200 at 20°K., 1/10 at 50°K., 1/6 at 100°K., and 1/4 at temperatures above 150°K.

As in the cases of thorium and gadolinium, the factor limiting the accuracy was the temperature measurement. Heat capacity values obtained from the smooth curve were thought to be accurate to ± 0.1 per cent down to 30°K. and to ± 1 or 2 per cent at 15°K.

DISCUSSION

Thorium

The value of the standard entropy of thorium, $S^{\circ}_{298.16}$, obtained in this research is 12.760 cal. deg.$^{-1}$ (g. atom)$^{-1}$. (Hereafter, these units of entropy will be represented by e.u.) This is contrasted with the value of 13.58 e.u. estimated by Lewis and Gibson.[2] Their value was based only on the average heat capacity between the temperatures of liquid hydrogen and liquid nitrogen, plus the assumption that the heat capacity of thorium behaved in a manner similar to several other metals. The discrepancy between these two values of entropy can certainly be attributed to inadequacies in the assumptions of Lewis and Gibson.

Thorium does not exhibit any anomalies in its heat capacity over the range 15-300°K. The deviation of the measured values from a smooth curve increased to ± 0.3 per cent in the range 135-155°K., but this is insignificant as compared with the anomalies exhibited by cerium[3] in the range 135-180°K. Likewise, in the temperature range over which it was studied, uranium[49] showed no anomalies in contrast to the behavior of neodymium.

Gadolinium

As can be seen from Figure 8, there is an anomaly in the heat capacity of gadolinium which reaches a maximum at 18.6°C. ± 0.3°. This corresponds closely to the Curie temperature of 16°C. ± 2.0° found by Urbain, Weiss, and Trombe,[4] and also to the values of 15.9°C. ± 0.1° and 17.7°C. ± 0.3° obtained by Elliott, Legvold, and Spedding[13] from experiments on remanent magnetization and magnetic susceptibility respectively. The shape of the heat capacity curve is similar to that found in the heat capacity studies of the other ferromagnetic elements, iron, cobalt, and nickel, in the neighborhood of their respective Curie temperatures.[39] These observations lead to the conclusion that the anomalous behavior is directly associated with the ferromagnetic phenomenon.

The quantitative interpretation of heat capacity data for ferromagnetics is still very rudimentary, and experiments of this type may, in time, serve as guides for future modification of theory. Nevertheless, it seems worthwhile to examine these results in light of existing theoretical schemes. It is of interest to compare: the magnetic entropy with its theoretical value, the heat capacity associated with the energy of magnetization with its value predicted from magnetization data alone, and the discontinuity of the heat capacity at the Curie temperature with theoretical predictions.

The measured heat capacity at constant pressure, C_p, may be regarded as the sum of several contributing factors, and may be written as:

$$C_p = C_q + C_m + C_e + \delta C \tag{15}$$

where C_q = the lattice heat capacity

C_m = the magnetic heat capacity

C_e = the electronic heat capacity

δC = the dilatation term, the difference between the heat capacities at constant pressure and at constant volume

Both C_m and C_e are electronic in origin, but are treated as distinct quantities. The following relation for S_p, the entropy associated with the measured heat capacity at constant pressure, is obtained from relations (12) and (15):

$$S_p = S_q + S_m + S_e + S_{\delta C} \tag{16}$$

where the same subscripts are retained. The separation in relations (15) and (16), while admittedly not rigorous, may form the basis for discussion, since to a first approximation the several terms are independent.

The value of C_q can be calculated as a function of temperature, assuming that it can be represented by the Debye function with a single value of θ_D, namely 152. This value was estimated from the lowest experimental values of the heat capacity, and was used to extrapolate the heat capacity curve from 0-15°K. (For arguments pertaining to the validity of this choice of θ_D, see the section on results.) Values of C_q can be obtained by the use of the tables of Beattie.[28] Numerical integration of these values from 0-360°K. gives a total lattice contribution to the entropy, S_q, of 13.115 e.u. With the previous assumption that the electronic contribution to the heat capacity is $C_e = 0.0016\ T$ cal. deg.$^{-1}$ (g. atom)$^{-1}$, the electronic entropy, S_e, is calculated as 0.576 e.u. at

360°K. The dilatation contribution to the heat capacity was shown to be zero below 20°C. and approximately 0.034 x T/298 cal. deg.$^{-1}$ (g. atom)$^{-1}$ above this temperature. The entropy contribution of the term, $S_{\delta C}$, at 360°K. is thus 0.007 e.u. Making use of the value of S_p in Table 7 and of relation (16), the value of S_m, the magnetic contribution to the entropy, is found to be 3.540 e.u. at 360°K.

The value of the magnetic entropy may now be compared with the predicted value. In the case of gadolinium, both the saturation moment and the paramagnetic susceptibility may be accounted for in the same manner as in the "ideal" dilute gadolinium salts.[50] Thus, the gadolinium atoms may be regarded as tripositive, and in the spectroscopic state $^8S_{7/2}$, which represents a parallel alignment of seven electrons in the 4 f shell. There are $2J + 1$ or eight energetically equivalent energy states for the tripositive atom. (Since $S = J$ in this case, there are also $2S + 1$ equivalent energy states.) When the atom is placed in a field, the energies of these eight states are split, depending upon the orientation of the atom in the field. In a ferromagnetic substance, the atomic moments are almost all lined up in one direction, which is equivalent to existing in one energy state. (Only at 0°K. are they completely lined up.) The entropy associated with the ferromagnetic state of gadolinium should be that for changing from one to eight possible energy states, R ln 8 or 4.132 e.u. The experimental value of the magnetic entropy was calculated to be 3.540 e.u., or 0.592 e.u. less than R ln 8. Since the values of C_p are still decreasing with increasing temperature at 360°K. there appears to be some magnetic contribution to the heat capacity, and entropy, above this temperature. In view of this fact, plus the uncertainties associated with the evaluation of S_e and S_q, the discrepancy of 0.592 e.u. is not disturbing.

In the formal Weiss treatment, which postulates the existence of an internal field of magnitude $N\rho\sigma$, the internal energy per gram associated with the intrinsic magnetization is $U = -\frac{1}{2}N\rho\sigma^2$. Assuming a constant density, the corresponding heat capacity is:

$$C_m = -AN\rho/2J \frac{\partial\sigma^2}{\partial T} \qquad (17)$$

where σ = the intrinsic magnetization per gram at temperature T

ρ = the density

N = the Weiss molecular field constant (not necessarily independent of temperature)

J = the Joule mechanical equivalent of heat

A = the atomic weight

From measurements of the paramagnetic susceptibility above the Curie temperature, it is possible to estimate $N\rho$. With the additional knowledge of $\partial\sigma^2/\partial T$ at various temperatures, it is then possible to evaluate the corresponding values of C_m and compare them with the more directly obtained values.

Kriessman and McGuire[40] have reported that the molar paramagnetic susceptibility may be represented as $\chi_M = 8.21/(T - 25.5)$, where T is measured in °C. On the basis of the Weiss theory, the gram susceptibility is given by the expression $\chi = C/(T - \theta) = C/(T - N\rho C)$. From the molar susceptibility given above, the Curie constant, C, is calculated to be 0.0524 per gram, and the value of $N\rho$ is then 5.70×10^3. Values of $\partial\sigma^2/\partial T$ in the range 8-14°C. may be estimated from the work of Elliott, Legvold, and Spedding.[13] From their curve the estimated values of $\partial\sigma^2/\partial T$ at 8, 10, and 14°C. are respectively -230, -290, and -507. Equation (17) then gives the values of magnetic heat capacity for 8, 10, and 14°C. as 2.5, 3.1, and 5.4 cal. deg.$^{-1}$ (g. atom)$^{-1}$. These may be compared with experimental values of 5.60, 5.85, and 6.46 cal. deg.$^{-1}$ (g. atom)$^{-1}$ obtained on the basis of relation (15).

The data of Kriessman and McGuire[40] for gadolinium allow the calculation of the effective magneton number, $\mu_{\text{eff.}}$, by the relation:

$$\mu_{\text{eff.}} = (3kC_m/B^2N)^{\frac{1}{2}}$$

where k = Boltzmann's constant

C_m = molar Curie constant

B = numerical value of Bohr magneton

N = Avagadro's number

The value of $\mu_{\text{eff.}}$ calculated for gadolinium from this equation is 8.15, which corresponds closely to the value of 7.94 calculated for a spin of 7/2 from the spin-only equation $\mu^2_{\text{eff.}} = 4S(S + 1)$.

The next item to be considered is the discontinuity in the heat capacity. Since the initially abrupt drop on the high-temperature side of the maximum glides into a more gradual decrease, it is customary to extrapolate back from that side and take the discontinuity as the difference between the maximum heat capacity and the extrapolated point. Such a procedure yields for the discontinuity a value of about 7 cal. deg.$^{-1}$ (g. atom)$^{-1}$, which is very similar to that found in the case of iron, and about 3.5 times that found for nickel. While the Weiss theory[41] comes close to agreement in the case of nickel, there is no such agreement for gadolinium.

The statistical theories of Firgau,[42] Takagi,[43] and Weiss,[44] which are based on the Ising model, are essentially equivalent. For simple cubic, body-centered, or face-centered cubic lattices the discontinuity in the heat capacity at the Curie temperature is found to be:

$$\Delta C = \frac{3R}{8} \frac{Z^2(Z - 2)}{Z \quad 1} \ln \frac{Z}{Z - 2}^{\,2} \text{ cal. deg.}^{-1} \text{ (g. atom)}^{-1}$$

where Z = the number of nearest neighbors.

It may be assumed that the value would not be essentially different for hexagonal closest-packing. For Z = 12, the discontinuity is 3.24 cal. deg.$^{-1}$ (g. atom)$^{-1}$, assigning one spin per atom. There seems to be no way to fit this to the case of gadolinium.

Measurements of the heat capacity of gadolinium in the range below 15°K. are desired since they would allow a better evaluation of θ_D, and, therefore, a better approximation to the true lattice heat capacity. They would also allow direct evaluation of the electronic contribution to the heat capacity of gadolinium, if this term can be assumed to vary linearly with the temperature in the range of these measurements.

Extension of the heat capacity measurements of gadolinium to higher temperatures is also desired for a better evaluation of the magnetic contribution to the entropy. As mentioned before, the decreasing values of C_p as the temperature increases at 360°K. indicate that some magnetic contribution to the heat capacity and entropy still exists above this temperature.

Erbium

There are three maxima in the heat capacity of erbium, as is shown in Figure 9. Results from various runs show the heat capacity to be reproducible in the vicinity of the maximum at 84°K. The results of run 4 show not only that the heat capacity curve is continuous through the maximum, but also that there is a region of about 1.2° at the very peak where the curve is almost flat.

A second maximum, at 53.5°K. ± 0.3°, exhibits a dependence on past thermal history of the sample. The heat capacity in the vicinity of the peak apparently is dependent upon the temperature to which the sample has been cooled prior to making measurements. However, the heat capacity seems completely reproducible when the sample is cooled to as low as 23.5°K. before making measurements in the region around 53.5°K.

The heat capacity in the region of the third maximum, at 19.9°K. ± 0.3°, is shown in Figure 10. The various runs made in this temperature range indicate that the lower the temperature to which the sample is cooled before the measurements are started, the higher is the peak of the maximum. Unfortunately, it was not possible to maintain the temperature of the lower reservoir and shield below 20°K. for sustained periods. Because of this, a thorough study on the dependence of the height and shape of the maximum as a function of the length of time the sample was maintained below 20°K. was not possible. From the data that were taken, it appears that the peak height and shape depend only on the temperature to which the sample is cooled before taking measurements and not on the length of time the sample is maintained at this temperature before taking measurements. However, the data are insufficient to permit a definite conclusion.

The temperatures of the maxima in the heat capacity curve correspond to those at which several other properties of erbium exhibit anomalous behaviors. The maximum at 84°K. corresponds roughly to the temperature of 80°K. where Legvold, et al.[16] reported a change in slope of the resistivity versus temperature curve. There is a slight bump in the initial magnetic susceptibility curve at 80°K. and a region between 65-80°K. where the magnetic susceptibility is independent of temperature. The results of the resistivity and magnetic susceptibility measurements suggest the possibility of a Néel point, i.e., a transition from paramagnetic behavior at higher temperatures to antiferromagnetic behavior at lower temperatures, in the region of 80°K. Koehler and Wollan[20] predicted from neutron diffraction that a magnetic transition, "the nature of which is unknown", sets in at about 80°K. These neutron diffraction studies would, at first, seem to support the possibility of a Néel point, but, as yet, attempts to interpret the data in terms of any model of antiferromagnetic order have been unsuccessful. The heat capacity curve of erbium around 84°K. shows little similarity to the heat capacity curves of known antiferromagnetic materials, such as MnF_2[45] and $NiCl_2$[46], around their Curie temperatures. Such a comparison should be made with reservations in this case, since two of the maxima in the heat capacity curve of erbium fall so close together that they have a tendency to mask each other.

A review of the properties of erbium in the region around 53.5°K. suggests nothing which would explain the maximum of the heat capacity. Elliott, Legvold, and Spedding[13] did find that the magnetic susceptibility becomes field dependent at 56°K. ± 5°, but this would not account for the heat capacity behavior. The possibility of anomalous electronic contributions to the heat capacity, as in the cases of cerium, praseodymium, and neodymium,[3] should be considered. At present, this appears to be the most likely way to account for the maximum at 53.5°K.

The maximum in the heat capacity at 19.9°K. corresponds to the temperature at which Elliott, Legvold, and Spedding[13] predicted the onset of ferromagnetism. They made no measurements of remanent magnetization, but based their opinion solely on magnetic susceptibility measurements. Koehler and Wollan[20] interpreted their neutron diffraction measurements as showing a definite ferromagnetic state at 4.2°K. The magnetic ordering, which they interpreted as ferromagnetic in nature, first appears as high as 35°K. and becomes more pronounced as the temperature is decreased. A change from an antiferromagnetic state to a ferromagnetic state does not alone afford a good explanation for a maximum in the heat capacity, since there should be no entropy change in going from one ordered state to another. However, it is possible that sharp changes in the other factors contributing to the heat capacity might accompany such a transition, thus accounting for a heat capacity maximum at the temperature of the transition. It was hypothesized by

Guillaud[47] that MnAs has a transition from antiferromagnetism to ferromagnetism, and an accompanying maximum is found in the heat capacity. Although the hypothesis accounted for the observed behavior of the other properties of MnAs, the maximum in the heat capacity was not explained. The maximum in the heat capacity of erbium at 19.9°K. may result from an electronic transition similar to those found for cerium and neodymium[3] in this same temperature range.

An evaluation of the entropy and heat capacity associated with each of the three maxima is impossible because the temperature ranges of the anomalous contributions overlap. However, it is possible to calculate an approximate value of the total entropy change associated with the three maxima.

This total entropy change may be calculated in the following manner. It is impossible to obtain a value of the Debye characteristic temperature, θ_D, for erbium from the low temperature heat capacity measurements. This is due to the fact that at these lowest temperatures the magnitudes of the magnetic and electronic contributions are unknown. For reasons presented earlier (see page 56), the best approximation to a value of θ_D for erbium should be obtained from linear extrapolation of the θ_D values of 132 for lanthanum and 152 for gadolinium. This gives a value of $\theta_D = 165$ for erbium, from which values of the lattice contribution to the heat capacity can be estimated using the Debye equation. A value of 11.710 e.u. at 300°K. is obtained for S_q, the lattice contribution to the entropy, from a table[48] of entropy versus θ_D/T. A value of

0.037 cal. deg.$^{-1}$ (g. atom)$^{-1}$ was calculated for $C_p - C_v$ at 300°K. in the section on erbium results. The entropy contribution of this term at 300°K. is 0.018 e.u. The electronic contribution to the heat capacity is assumed to be the same as in lanthanum,[3] namely, $1.6 \times 10^{-3}T$cal. deg.$^{-1}$ (g. atom)$^{-1}$. The corresponding entropy contribution is 0.480 e.u. Using equation (16) and the measured value of 17.634 e.u. for the total entropy, the magnetic entropy at 300°K. is calculated to be 5.426 e.u.

A theoretical value of the magnetic entropy can be obtained if the atoms of erbium in the metal are regarded as tripositive, and are assigned the same spectroscopic state as that of the free ion, namely, $^4I_{15/2}$. (The valence electrons are regarded as being paired in the bonding band and not contributing to the magnetic moment.) At 0°K. all of the atoms would be in the lowest energy state of the possible $2J + 1$ or 16 states. At sufficiently high temperatures, the atoms will assume a random distribution among the 16 possible states. The entropy change associated with the change from 1 to 16 possible energy states is R ln 16 or 5.382 e.u. This simplified treatment of the actual metal can be treated by comparing predicted and experimental values of S_m, the magnetic entropy. The splendid agreement between the two values, 5.382 and 5.426 e.u., appears fortuitous considering the assumptions involved in approximating the lattice and electronic contributions to the entropy. Nevertheless, the agreement leads to confidence in the method used to obtain the predicted value of S_m.

An extension of the work on erbium should include measurement of the heat capacity in the range 1-25°K. From these measurements it should be possible to obtain better values for the Debye characteristic temperature and also for the electronic heat capacity. Hence, better values for the lattice and electronic contributions to the entropy could be determined. A thorough investigation of the 19.9°K. maximum should be made in order to determine its dependence on the previous thermal history of the sample. There is apparently a large magnetic contribution to the heat capacity at 15°K., and this can reasonably be assumed to extend below 15°K. Investigation of the heat capacity in the proposed range should indicate the nature of the magnetic contribution below 15°K. Another interesting extension of this work would be a combined heat capacity and magnetic study from 1-90°K. in order to determine the heat capacity of the sample as a function of applied magnetic field. This should help in determining the relationship between the heat capacity and magnetic properties of erbium.

Measurements to determine remanent magnetization might clear up some of the vagueness which now surrounds the existence and temperature region of a ferromagnetic state. Magnetic susceptibility measurements on a single crystal of erbium might provide information to support the hypothesis of antiferromagnetism in erbium. Koehler and Wollan[20] have proposed neutron diffraction measurements in conjunction with an applied magnetic field. Elliott, Legvold, and Spedding[13] have measured the magnetic susceptibility of dysprosium and have shown that it behaves in a manner similar to that of erbium. Its magnetic properties are more distinct and the transitions occur farther apart, so that a comparison of its heat capacity with that of erbium might be helpful in the interpretation of the behavior of the latter.

General

The rare earth metals might reasonably be expected to have Debye characteristic temperatures which would be close together and show a monotonic variation with atomic number. Such a behavior would be in keeping with the increasing atomic weight and generally decreasing atomic volume experienced in going from lanthanum to lutetium. The characteristic temperature, θ_D, is related to the characteristic frequency, V_D, by the relation $hV_D = k\theta_D$, where h and k are respectively the Planck and Boltzmann constants. This characteristic frequency is related to the force constant F and density ρ by the relation $V_D = (F/\rho)^{\frac{1}{2}}$. The force constants of the rare earth metals would be expected to increase as the atomic number increases because of the decrease in atomic volume and resultant tighter bonds. The density also increases as the atomic number is increased. Since it is not known whether F or ρ has the greater percentage change, the trend of the θ_D values must be experimentally determined. The values of $\theta_D = 132$ for lanthanum[3] and $\theta_D = 152$ for gadolinium, which were determined thermally, show that the force constant is the dominating factor. As mentioned previously, the main interest in the values of θ_D has been for prediction of lattice heat capacities, so the values of θ_D determined thermally rather than from sound velocities have been used. The values of θ_D determined from sound velocity measurements[33] are 162 for lanthanum, 176 for gadolinium, 182 for dysprosium, and 192 for erbium. Although these absolute values have not been used, they do show the expected monotonic change with atomic number and also show this change to be roughly linear. It should be mentioned that the determination of lattice heat capacities by a single value of θ_D is only approximate, since the assumptions used in derivation of the Debye equation are only approximate.

The good agreement of the predicted and experimental values of the magnetic entropy of erbium at 300°K. and the approximately linear change in the lattice heat capacities of the rare earth metals suggested that the entropies of the other rare earth metals might be predicted. These predictions were made in the following manner. The θ_D values are assumed to vary linearly in going from lanthanum to lutetium, and are determined by the values of $\theta_D = 132$ for lanthanum and $\theta_D = 152$ for gadolinium. The electronic contribution to the heat capacity is assumed to be constant throughout the series, and equal to that in lanthanum, namely, $.0016T$ cal. deg.$^{-1}$ (g. atom)$^{-1}$. There is no justification for this except that it appears to be the only approximation that can be made. The magnitude of $C_p - C_v$ is considered negligible in light of the small values calculated for gadolinium and erbium. The magnetic contribution to the entropy is calculated assuming that the atoms exist as the tripositive ion in the metal, and that the only entropy contributed by the valence electrons is in the electronic heat capacity. This is equivalent to the assumption used in the case of the "ideal" magnetically dilute rare earth salts. At 0°K. the ions are assumed to exist in the lowest energy state of the $2J + 1$ possible states.

At 300°K. the ions are assumed to be randomly distributed in all of the possible 2J + 1 energy states. The entropy associated with the distribution of the ions into the available energy states as the metal is warmed from 0-300°K. is R ln (2J + 1). The success of this treatment in the case of erbium seems to justify its use.

Although these assumptions lead to valid predictions for most of the rare earth metals, they would be inadequate in the cases of europium, ytterbium, and possibly samarium because of the abnormal valence states and resulting loose bonding exhibited by these metals. In their salts, both europium and ytterbium are known to exist preferentially in the divalent state, with the 4 f shell respectively half-filled and completely-filled. This tendency is presumed to carry over into the metals, where the atoms possess the same electron core as the dipositive ion. The looser binding in the case of the dipositive ions should cause the θ_D values of europium and ytterbium to be considerably smaller than the other rare earth metals and, hence, at any particular temperature their lattice contributions to the heat capacity and entropy would be larger.

In the case of europium, the divalent ion is in the spectroscopic state $^8S_{7/2}$, and would, therefore, be expected to have a magnetic contribution to its entropy equal to that for gadolinium. Because the lattice contribution to the entropy is expected to be abnormally large, europium would be expected to have an entropy greater than its neighbors, samarium and gadolium. In the case of ytterbium, the divalent ion is in the spectroscopic state $^1S_0$, and would be expected to have no magnetic contribution to the entropy. Because of the anticipated abnormally large lattice entropy, ytterbium would be expected to have a total entropy somewhat larger than lutetium.

Table 11 and Figure 12 show the results of the calculations.

Table 11

Predicted and experimental values of S^o_{300} for the rare earth metals

Element	θ_D	$S_q + S_e$ e.u.	J[a]	R ln (2J+1) e.u.	Pre. S_p	Exp. S_p
La	132	13.41	0	0	13.41	13.64[b]
Ce	135	13.29	5/2	3.56	16.85	16.68[b]
Pr	138	13.16	4	4.37	17.53	17.49[b]
Nd	141	13.04	9/2	4.57	17.61	17.54[b]
Pm	144	12.92	4	4.37	17.29	- -
Sm	147	12.80	5/2	3.56	16.36	- -
Eu	- -	- -	7/2	4.13	- -	- -
Gd	152	12.57	7/2	4.13	16.70	15.83
Tb	155	12.44	6	5.10	17.54	- -
Dy	159	12.32	15/2	5.51	17.83	- -
Ho	162	12.20	8	5.63	17.83	- -
Er	165	12.08	15/2	5.51	17.59	17.52 ~~17.63~~
Tm	168	11.95	6	5.10	17.05	- -
Yb	- -	- -	0	0	- -	- -
Lu	174	11.71	0	0	11.71	- -

[a] The total angular momentum quantum number of the tripositive ion, except for europium and ytterbium where J is for the dipositive ion.

[b] These experimental values of S_p were obtained from reference 3.

Figure 12

Predicted and experimental values of S^{o}_{300} for the rare earth metals

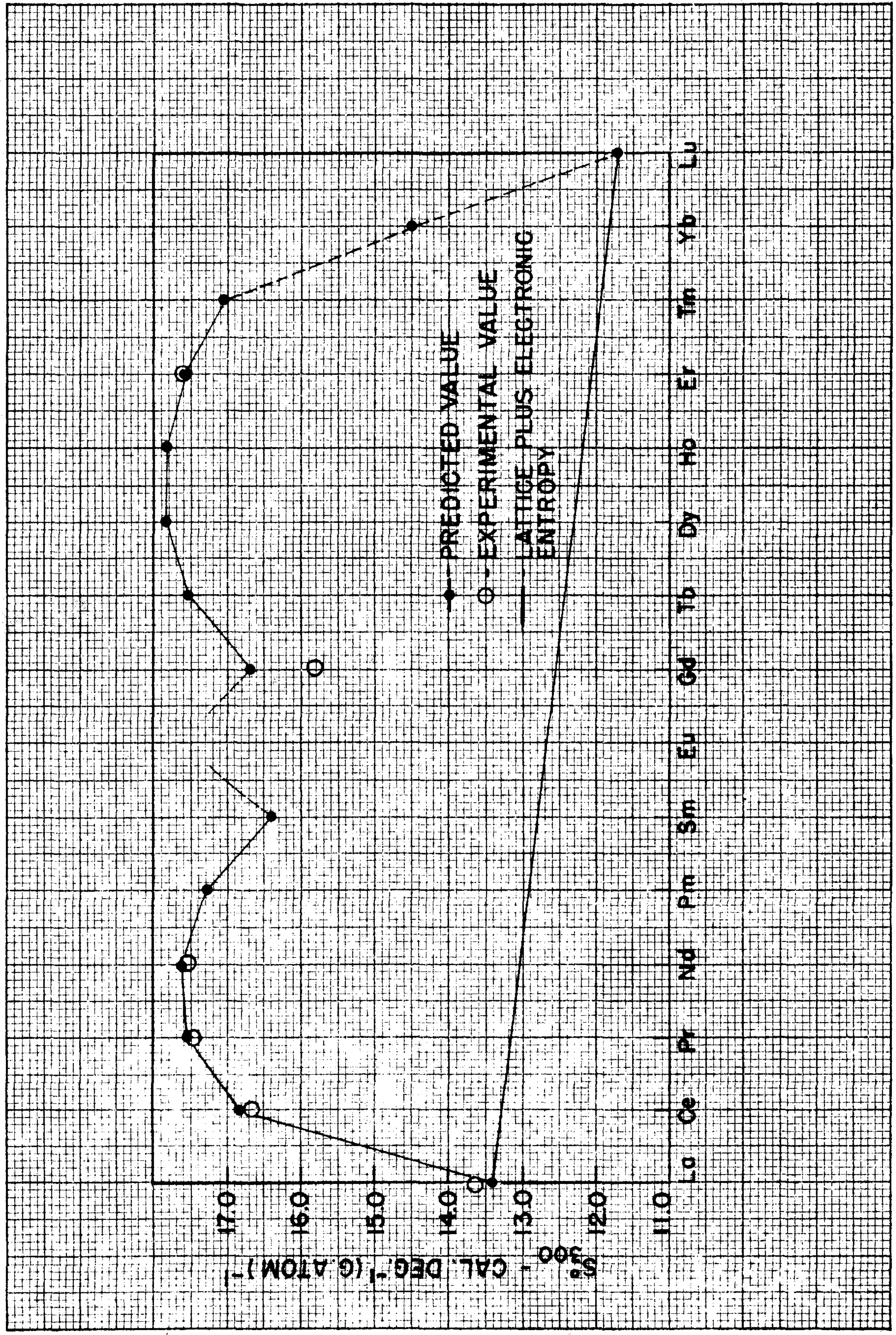
S°300 - CAL. DEG.⁻¹ (G. ATOM)⁻¹
17.0
16.0
15.0
14.0
13.0
12.0
11.0
La
Ce
Pr
Nd
Pm
Sm
Eu
Gd
Tb
Dy
Ho
Er
Tm
Yb
Lu
● - PREDICTED VALUE
○ - EXPERIMENTAL VALUE
— LATTICE PLUS ELECTRONIC ENTROPY

There seems to be exceptional agreement in most cases between the theoretical and experimental values of entropy. The one exception is gadolinium, but this would not be expected to agree at 300°K. A part of the magnetic contribution to the entropy still remains above this temperature, and this would seem to account for the fact that the entropy of gadolinium is 0.9 e.u. lower than predicted at 300°K. Parkinson, Simon, and Spedding[3] previously observed that the magnetic entropy of praseodymium was of the order of R ln 9, but they did not obtain the expected values for cerium and neodymium.

The experimental measurement of the heat capacity of lutetium from 1-300°K. would provide a test of the assumptions concerning both the behavior of θ_D and the electronic heat capacity. Should eventual experimental data for dysprosium confirm the predicted value, this would bolster the confidence in the adequacy of the underlying assumptions.

SUMMARY

A description of the construction and operation of an adiabatic calorimeter for use in the temperature range 15-300°K. has been presented, and the methods used in the treatment of data and calculation of results have been discussed.

The heat capacity of thorium was measured from 15-300°K., and the thermodynamic functions were calculated for the range 0-300°K. No anomalies were observed in the heat capacity of thorium over this temperature range.

The heat capacity of gadolinium was measured from 15-355°K., and the thermodynamic functions were calculated for the range 0-355°K. An enhanced heat capacity associated the the ferromagnetic behavior was observed, with a maximum at 18.6°K. The heat capacity, heat capacity discontinuity, and entropy associated with the magnetic phenomenon were determined from the results and they have been discussed in connection with theories of magnetism.

The heat capacity of erbium was measured from 15-320°K., and the thermodynamic functions were calculated in the range 0-320°K. Three maxima were observed in the heat capacity curve of erbium, at 19.9, 53.5, and 84°K. The maxima at 19.9 and 53.5°K. were found to be dependent upon the previous thermal history of the sample, and this dependence was investigated. The three heat capacity maxima have been discussed and compared with anomalous behavior of other properties of erbium. The entropy

associated with the combined anomalies was determined and compared with the theoretical value.

The Debye characteristic temperatures were found to increase from 132 to 152 in going from lanthanum to gadolinium. This trend in θ_D values has been discussed.

A method of predicting the entropies at higher temperatures of the other rare earth metals has been presented and the predicted values shown. Comparison of the predicted values with experimental values showed very good agreement between the two.

LITERATURE CITED

1. Desorbo, W., J. Chem. Phys., 21, 876 (1953).
2. Lewis, G.N. and Gibson, G.E., J. Am. Chem. Soc., 39, 2554 (1917).
3. Parkinson, D.H., Simon, F.E., and Spedding, F.H., Proc. Roy. Soc. (London), A207, 137 (1951).
4. Urbain, G., Weiss, P., and Trombe, F., Compt. rend., 200, 2132 (1935).
5. Néel, L., Z. Elektrochem., 45, 378, (1939).
6. Dewar, J., Proc. Roy. Soc. (London), A89, 158 (1913).
7. Kelley, K.K., U.S. Bureau of Mines Bulletin No. 477, Washington, 1950.
8. "Selected Values of Chemical Thermodynamic Properties," National Bureau of Standards Circular No. 500, Washington, 1952.
9. Lawson, A.W. and Tang, Ting-Yuan, Phys. Rev., 76, 301 (1949).
10. Schuch, A.F. and Sturdivant, J.H., J. Chem. Phys., 18, 145 (1950).
11. Koenigsberg, E., Unpublished Ph.D. Thesis, Iowa State College Library, Ames, Iowa, 1952.
12. Trombe, F., Ann. Physique, Ser. 11, 7, 385 (1937).
13. Elliott, J.F., Legvold, S., and Spedding, F.H., Phys. Rev., 91, 28 (1953).
14. Barson, F., Legvold, S., and Spedding, F.H., U.S. Atomic Energy Commission Report ISC-424, August, 1953.
15. Trombe, F., and Foex, M., Compt. rend., 235, 42 (1952).
16. Legvold, S., Spedding, F.H., Barson, F., and Elliott, J.F., Rev. Modern Phys., 25, 129 (1953).
17. Kevane, C.J., Legvold, S., and Spedding, F.H., Phys. Rev., 91, 1372 (1953).

18. Banister, J.R., Legvold, S., and Spedding, F.H., to be published in *Phys. Rev.*

19. Elliott, J.F., Legvold, S., and Spedding, F.H., Unpublished Data, Ames Laboratory of the U.S. Atomic Energy Commission, Ames, Iowa, 1954.

20. Koehler, W.C., and Wollan, E.O., U.S. Atomic Energy Commission, ORNL-1620, p. 27, December, 1953.

21. Spedding, F.H., Fulmer, E.I., Butler, T., Gladrow, E., Gobush, M., Porter, P., Powell, J., and Wright, J., *J. Am. Chem. Soc.*, *69*, 2812 (1947).

22. Spedding, F.H. and Daane, A.H., *J. Am. Chem. Soc.*, *74*, 2783 (1952).

23. Blue, R.W. and Hicks, J.F.G., *J. Am. Chem. Soc.*, *59*, 1962 (1937).

24. Ruehrwein, R.A. and Huffman, H.M., *J. Am. Chem. Soc.*, *65*, 1620 (1943).

25. Scott, R.B., Meyers, C.H., Rands, R.J. Jr., Brickwedde, F.G., and Bekkedahl, N., *J. Research Nat'l. Bur. Standards*, *35*, 45 (1945).

26. Giauque, W.F. and Meads, P.F., *J. Am. Chem. Soc.*, *63*, 1897 (1941).

27. Nernst, W. and Lindemann, F.A., *Z. Elektrochem.*, *17*, 817 (1911).

28. Beattie, J.A., *J. Math. and Phys.*, *6*, 1 (1926).

29. Manly, W.D., "Thorium," Metallurgy Division, Oak Ridge National Laboratory, July 1, 1949.

30. Reynolds, M.B., U.S. Atomic Energy Commission, AECD-3242, May, 1951.

31. Bridgman, P.W., *Proc. Am. Acad. Arts Sci.*, *62*, 207 (1927).

32. Erfling, H.D., *Ann. Physik*, *41*, 467 (1942).

33. Carlson, C.E. and Smith, J.F., Unpublished Data, Ames Laboratory of the U.S. Atomic Energy Commission, Ames, Iowa, 1954.

34. Bridgman, P.W., *Proc. Am. Acad. Arts. Sci.*, *82*, 99 (1953).

35. Klemm, W. and Bommer, H., *Z. anorg. u. allgem. Chem.*, *231*, 138 (1937).

36. Bridgman, P.W., *Proc. Am. Acad. Arts Sci.*, *83*, 1 (1954).

37. Hoge, H.J. and Brickwedde, F.G., J. Research Nat'l. Bur. Standards, 22, 351 (1939).

38. Hoge, H.J., Rev. Sci. Instr., 21, 815, (1950).

39. Kelley, K.K., U.S. Bureau of Mines Bulletin No. 476, Washington, 1949.

40. Kriessman, C.J. and McGuire, T.R., Phys. Rev., 90, 374 (1953).

41. For development of the equations see Becker, R. and Doring, W., "Ferromagnetismus," p. 67, Julius Springer, Berlin, 1939.

42. Firgau, U., Ann. Physik, 40, 295 (1941).

43. Takagi, Y., Proc. Phys. Math. Soc. Japan, 23, 553 (1941).

44. Weiss, P.R., Phys. Rev., 74, 1493 (1948).

45. Stout, J.W. and Adams, H.E., J. Am. Chem. Soc., 64, 1535 (1942).

46. Busey, R.H. and Giauque, W.F., J. Am. Chem. Soc., 74, 4443 (1952).

47. Guillaud, C., J. phys. radium, 12, 223 (1951).

48. Bornstein, Landolt, "Physikalische-Chemische Tabellen," Erste Ergänzunband, p. 707, Julius Springer, Berlin, 1927.

49. Jones, W.M., Gordon, J., and Long, E.A., J. Chem. Phys., 20, 695 (1952).

50. Pauling, L., Proc. Natl. Acad. Sci. U.S., 39, 551 (1953).

51. Osborne, N.S., Stimson, H.F., Sligh, T.S. Jr., and Cragoe, C.S., Bur. Standards Sci. Paper, 20, 65 (1925).

ACKNOWLEDGMENTS

The author wishes to express his appreciation to Dr. Maurice Griffel for his guidance and advice in this research. The author wishes to acknowledge the benefit of discussions with Dr. R. E. Rundle on the interpretation and presentation of these data and the discussions with Dr. F. H. Spedding on the interpretation of the data. The author also wishes to thank the following persons: Dr. Jack Powell for preparation of the rare earth salts; Mr. Karl Gschneidner and Mr. David Dennison for preparing the metals; the analytical section of the Ames Laboratory, especially the spectrographic section, for the analyses of the metals; and Mr. Lloyd Hanson for assistance in some of the measurements and calculations.